THE UNIVERSITY OF CHICAGO

PARALLEL ROLES FOR CDX AND RETINOIC ACID IN THE REGULATION OF THE PECTORAL FIN FIELD IN THE EARLY ZEBRAFISH EMBRYO

A DISSERTATION SUBMITTED TO

THE FACULTY OF THE DIVISION OF THE BIOLOGICAL SCIENCES

AND THE PRITZKER SCHOOL OF MEDICINE

IN CANDIDACY FOR THE DEGREE OF

DOCTOR OF PHILOSOPHY

COMMITTEE ON DEVELOPMENT, REGENERATION AND STEM CELL BIOLOGY

BY

CHRISTOPHER A. QUINTANILLA

CHICAGO, ILLINOIS

JUNE, 2020

“Stare, pry, listen, eavesdrop. Die knowing something. You are not here long”

- Walker Evans

TABLE OF CONTENTS

LIST OF FIGURES

ACKNOWLEDGEMENTS

Culver Hall felt like home and I'm very appreciative for all the people I met. Thank you, Dr. Robert Ho for always leaving your door open. I appreciated your approachable demeanor and the freedom you gave me to pursue what interested me. Thank you, Dr Vicky Prince for all your thoughtful comments and encouraging words after presentations. I appreciate all the encouragement supportiveness of my committee members Dr. Munro, Dr. Ragsdale and Dr. Horne-Badovinac. To my lab mates: Stephanie, you have soo much positive energy and optimism, I really appreciated your company and the help you gave me. Erin and Lindsey, your supportive demeanor and productivity were inspiring. Thank you to Adam and Alana for all your helpful conversations and for all making my work around the lab possible. Haley, I always admired your curiosity for science and your thoughtful questions during talks. To members of the Prince lab: thank you for your willingness to help at all times. Manny and Ana, your feedback on presentations and on my writing were very helpful. Thank you to past members of the Ho lab Jessie and Qiyan who encouraged me to join the lab. To my dear classmates: Kamil, Younan and Claire, I was always inspired by your brilliance and even more by your compassion. Thank you for your friendship, I aspire to be more like you every day. Thank you to all my housemates at Bowers that filled me with warmth and comfort after long days in the lab. And to my parents Yanira and Fernando, you filled me with a powerful desire to work hard and pursue an education. I love you.

CAQ

March, 2020

Chicago

ABSTRACT

The factors that determine the precise antero-posterior (AP) position of the vertebrate limb are still unknown. This dissertation focuses on examining the roles of two classes of molecules in regulating the (AP) position of the pectoral fins in zebrafish. The pectoral fin is the fish homolog of the tetrapod forelimb. Retinoic acid (RA), one of the two molecules I investigate in this dissertation, must be carefully regulated in order for a fin bud to form and subsequently for it to establish normal AP polarity. RA is also required for the pectoral fin field to form, but the mechanistic role RA plays in development of the fin field is not clear. In this study, I describe the role for RA in regulating the precise location of the fin field. I also characterize the role that the Cdx family of transcription factors play in regulation of the pectoral fin field. I specifically examine two paralogs, Cdx4 and Cdx1a, that have never been studied in the context of pectoral fin development but are known to play a role in regulating cell fates along the AP axis. As I demonstrate, during gastrulation RA and the Cdx transcription factors play a parallel role in restricting the antero-posterior location where the pectoral fin field forms.

CHAPTER 1

INTRODUCTION

1.1 Prologue

This work is dedicated to advancing our understanding of how the vertebrate forelimb forms at precise locations along the body. Studies in *amblystoma* over a century ago first showed that the progenitor cells that eventually give rise to the forelimb are established much earlier in development compared to when the forelimb is first visible [1]. When transplanted to another region, this group of progenitors later gave rise to ectopically positioned limbs. This special group of cells in the early embryo that eventually gives rise to vertebrate limb will be referred to as the limb field.

Today, there is a detailed understanding of how signals coordinate growth and patterning of the skeletal elements in the limb. However, we still lack a clear understanding of how forelimb position along the body is regulated. In tetrapods, variation in forelimb position is believed to be due primarily to changes in where the limb precursors form since the limb field and limb bud are positioned at a similar AP level. In zebrafish, the position of the pectoral fin field is first established, and these cells then converge to a smaller region within the fin field. Thus, the initial area where the limb field forms is critical in determining where the limb bud forms. In contrast the variation in position of pelvic fins in different fish is believed to be due to differences in where the field migrates. Changes in yolk surface area and active migration leads to substantial deviations in where pelvic fin progenitors form and where the pelvic fin buds later end up. In this study, I seek to identify potential regulators of the fin field and identify the time of development when pectoral fin position is determined.

In this chapter, I will first discuss the similarities between the fins of fish and the limbs of tetrapods. I will then discuss two potential regulators of the earliest steps of pectoral fin development. First, I will introduce the signaling molecule called retinoic acid (RA). Although RA has been extensively studied for its powerful effects on gene expression and development in the vertebrate embryo, there is still disagreement on how RA regulates developmental processes. I will also discuss how the RA distribution in the embryo is regulated by highlighting key steps in the synthesis and degradation process that are key for understanding how I eventually manipulated the pathway in my studies. Lastly, I will describe some of the powerful effects on development when RA is mis-regulated. Studies on forelimb and hindbrain patterning have led to different models for how RA ultimately acts in regulation of developmental processes.

The Cdx family of transcription factors are the second class of regulators I will be discussing. They play important regulatory roles during development by directly binding to DNA and controlling gene expression. I will highlight some of the different mechanisms by which the Cdx transcription factors regulate patterning along the AP axis. Cdx factors also interact with the RA pathway. These mechanisms also serve as a template for understanding how Cdx transcription factors may ultimately regulate forelimb positioning.

Lastly, I will discuss why Cdx transcription factors and RA are ideal candidates for regulation of forelimb position. The key transcription factor, Tbx5a and *Hox* genes have been implicated in the early regulation of the limb field. RA and the Cdx transcription factors are known to be direct regulators of *Hox* genes and may also regulate *tbx5a* directly. Here, I investigate whether RA and the Cdx transcription factors interact during formation of the fin field. My findings show that RA and Cdx act in parallel to regulate the fin field in zebrafish.

1.2 Paired limbs are homologous to paired fins

The paired limbs of tetrapods are locomotory organs that include both the forelimbs and hindlimbs. The general anatomical pattern of skeletal elements that form along the proximo-distal (PD) axis of tetrapod limbs are similar. Paired limbs are also similar to the paired fins of fish because they each evolved from the paired fins of a common ancestor [2], [3]. For this reason, limbs and fins are homologous structures. In particular, the pectoral fins of fish are homologous to the forelimbs of tetrapods and the signaling molecules that regulate development of the forelimbs and pectoral fins are conserved [4], [5].

A hierarchy of steps occur during forelimb development beginning with specification of a limb field in the embryo that later resides in a specific antero-posterior region of the embryo called the lateral plate mesoderm (LPM) (this will be discussed in more detail in section 1.5) [5]. The LPM resides just lateral to the somitic mesoderm and extends along the antero-posterior (AP) axis of both the left and right sides of the embryo. The limb field later gives rise to a small bud of LPM cells that protrude from the trunk and are covered by a layer of ectodermal cells that eventually thickens into a structure called apical ectodermal ridge (AER) [5]. The AER becomes a signaling center at the distal end of the limb bud that specifies the PD axis while a different signaling center at the posterior region of the limb bud called the zone of polarizing activity (ZPA) specifies the (AP) axis of the limb bud [6]. These signals act along their respective axis to pattern the forelimb but they also act on each other to form a self-regulatory feedback loop that drives the growth of the limb bud [6]. As a result, patterning and growth of the fin bud become closely linked.

Zebrafish are small vertebrates and are particularly useful for studies related for forelimb development because the pectoral fins are already visible by 30 hours post fertilization (hpf) while in other vertebrates such as mice, the limb bud doesn't form until embryonic day 9 (E9). Zebrafish are also optically transparent as embryos, which is important for visualizing the behavior of the fin field cells before the fin bud forms. Importantly, the pre-limb bud stages of development are relatively less understood compared to the stages that occur after the limb bud forms. In the next section, I will introduce RA, a necessary signal for stages of early pectoral fin development before the fin bud forms.

1.3 Retinoic acid

1.3.1 How RA controls transcription

Retinoic acid (RA) is a small lipophilic molecule derived from retinol/vitamin-A that is thought to regulate development specifically in chordates through effects on gene expression [7]. In contrast to many of the known developmental signaling pathways that involve cell surface protein receptors, RA can instead bypass the cell membrane and bind to nuclear receptors, either retinoic acid receptors (RAR) or retinoid receptors RXR [8], [9]. Through these nuclear receptors, RA then regulates gene expression.

Nuclear receptors RAR and RXR bind specific sequences called retinoic acid response elements (RAREs). The conventional response to RA binding is transcriptional activation. Following RA binding to RARs, a conformational change results in dissociation of pre-existing repressive complexes and is followed by subsequent recruitment of Nuclear Co-activators/Steroid Receptor Coactivators (NCOA or SRC) 1-3, which can then promote histone

acetylation, opening of compact chromatin and recruitment of chromatin remodeling complexes to promote transcription [10], [11], [12], [13], [14].

There are also examples where RA binding instead leads to recruitment of repressive complexes such as PRC2, to promote gene repression. RA leads to gene silencing in the caudal progenitor zone which mediates axial elongation, the hindbrain and formation of the growth plate of the developing mouse limb [10], [15], [16], [17]. Together, these studies show that although RA primarily acts as an activator, RA could also act as a repressor in developmental processes.

1.3.2 The regulation of RA in the embryo

In zebrafish, multiple enzymatic steps establish the distribution of the active form of RA but the distribution is best predicted by the location of two class of enzymes that mediate limiting steps in the RA pathway. The first is the group of retinaldehyde dehydrogenase enzymes (Raldh1, Raldh2 and Raldh3). During zebrafish gastrulation, embryonic RA is primarily synthesized by the activity of Raldh2 (also called Aldh1a2) [18]. The second group of enzymes is the Cyp26 family of cytochrome P450 enzymes which are responsible for oxidation of RA into inactive forms (4-oxo-RA, 18-hydroxy-RA, 5-8-epoxy-RA or 4-hydroxy-RA). This results in downregulation of the RA pathway (reviewed in [7]). During zebrafish gastrulation, Cyp26a activity is responsible for most of the RA degradation activity.

Further, there are feedback mechanisms, depending on the regulation of *cyp26a* and *aldh1a2,* that prevent fluctuations where levels of RA become too high or too low. In mice and zebrafish, excess doses of ectopic RA treatment leads to later downregulation of *aldh1a2/Raldh2* expression and thus reduced RA synthesis [19], [29]. Negative feedback is also built in through regulation of *rdh10* an alcohol dehydrogenase that acts in synthesizing the aldehyde substrate

RALDH2 ultimately acts on to synthesize RA [20], [21], [22]

Cyp26a is a downstream target of RA such that increased levels of RA leads to an upregulation of *cyp26a*. The *cyp26a* promoter region is directly regulated by 2 RAREs, one near the promoter and a 2nd that is located 2kb upstream [23], [24]. In response to exogenous RA, *CYP26a* is upregulated in specific embryonic tissues such as the cranial region of quail, mouse and zebrafish [25], [26], [27]. This ultimately leads to a reduction of overall levels of RA. For this thesis, it is important to highlight that beads soaked in low concentration of RA comparable with what is seen at physiological levels can induce *cyp26a* [28]. There are also downstream targets of RA such as Fgfs that regulate *cyp26a*, suggesting an additional form of indirect feedback [28], [29].

Together, these feedback mechanisms often result in difficult to interpret results where excessively high levels of exogenous RA treatments lead to paradoxical phenotypes resembling the effects of excess and deficient RA conditions. This highlights the difficulty in interpreting the effects on RA signaling and the importance of disrupting RA signaling through milder approaches as I later describe in chapter 3.

The distribution of RA in the embryo can be manipulated by drugs that specifically target the activity of either the Aldh1a or Cyp26 family of enzymes. Talarozole, a small molecule can increase levels of RA in the embryo. This drug acts as an inhibitor of Cyp26 activity. Similar drugs such as ketoconazole also increase RA levels through the same mechanism. Diethylaminobenzaldehyde (DEAB), acts on the Aldh1a2 activity, resulting in depletion of RA. Related drugs can also act at the level of the nuclear receptors resulting in loss of RA signaling. Given the short half-life of RA these drugs have rapid effects on gene expression

In the work I later show, the distribution of *aldh1a2* and *cyp26a* expression are critical in assessing the normal distribution of RA. Changes to the activity of these are expected to result in severe effects on the overall distribution of RA.

1.3.3 Gradients of RA in the embryo

Although diffusible molecules are widely believed to form reliable gradients in developing embryos, the inability to visualize RA directly during early development makes it hard to know when an RA gradient is first established in zebrafish [30]. The earliest transgenic zebrafish reporter confirmed that at the tailbud stage (immediately post-gastrulation) levels of RA are high in the trunk and low at the head and tail regions [31]. Later in development, less sensitive RA reporters are able to detect traces of a gradient near the hindbrain region [28]. The RA gradient for the hindbrain and an additional presumed gradient in the limb bud is illustrated in (Fig.1.1). As with the hindbrain region, the limb bud has an expression domain of *aldh1a2* and *cyp26a* in close proximity to suggest that a gradient of RA forms [32].

The RA gradient in the developing limb bud runs across the proximo-distal (PD) axis. During embryonic stages when the limb bud is visible, RA is produced in the somites. This results in a high RA region (indicated in yellow). The proximal limb bud is exposed to highest levels of RA, since it is the closest to the somites. As a result, the relative levels of RA in the limb bud drop near the distal regions of the limb bud. This drop occurs due to growth distancing from the RA source in the somites and the expression of *cyp26b* in the distal end which clears the region of RA.

In the developing hindbrain, the RA gradient runs across the AP axis, along the rhombomere segments (shown in Fig.1.1 B). The hindbrain is divided into 8 segments

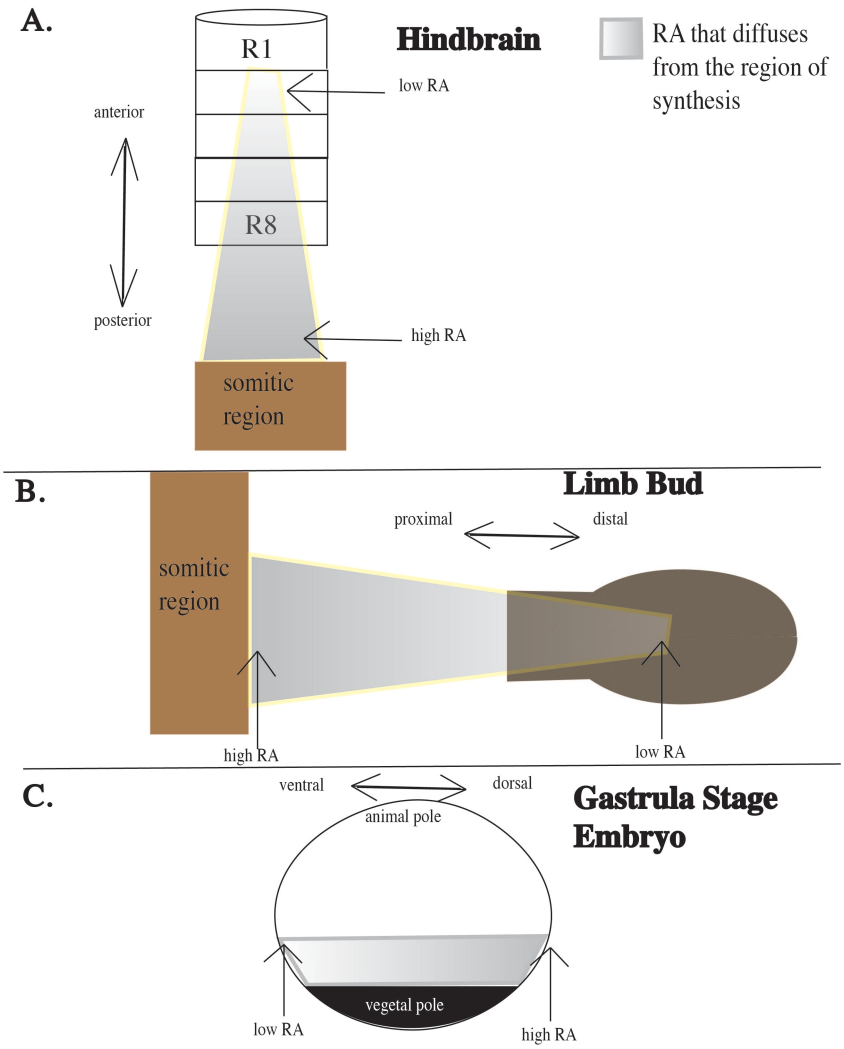

Fig.1.1 Presumed gradients of RA during development. (A) Illustration of a lateral view of the right forelimb bud and the adjacent somitic region. A gradient of RA (yellow) forms in the proximal limb bud as RA is synthesized in the somitic region (brown) and diffuses laterally towards the fin bud (black). Levels of RA are highest at the proximal limb bud and absent in the distal limb bud, due to degradation by Cyp26b). (B) Illustration of the dorsal hindbrain region during segmentation stages. RA from the somitic region (brown) diffuses rostrally to form a gradient of RA across the developing rhombomeres of the hindbrain (orange blocks). RA levels are highest at rhombomere 8 (R8) and lowest at rhombomere 1 (R1) due to Cyp26. (C) Illustration of the left side of a zebrafish embryo during late gastrulation. RA is synthesized near

Fig.1.1 (continued) the dorsal marginal zone (purple) and diffuses towards the ventral margin where RA levels are the lowest.

(rhombomeres 1-8). Rhombomere 8 is the most posterior segment and is closest to the paraxial mesoderm where RA is synthesized, while rhombomere 1 is the furthest. In addition, *cyp26a* is expressed in the anterior neuroectoderm region, anterior to rhombomere 1. Together, this results in a decreasing RA gradient from rhombomere 8 to rhombomere 1.

The earliest gradient of RA may be established as early as gastrulation in the zebrafish embryo. The expression pattern of *cyp26a* and *aldh1a2* at this stage suggests an RA gradient may actually form along the dorso-ventral (DV) axis which corresponds closely to the emerging AP axis [33]. The heart, pectoral fin, and kidneys each vary in sensitivity to RA and were fate-mapped to different regions along this presumptive DV gradient of RA. Highest levels of RA were at the dorsal end and lowest levels at the ventral end. Unfortunately, there is no RA reporter sensitive enough to detect the potentially low concentration of RA in the gastrula. Given how accurately the relative pattern of *cyp26a* and *aldh1a2* reflect an RA gradient at later stages, their expression suggests a gradient is also established by the mid to late gastrulation stage.

1.3.4 The range of developmental defects associated with mis-regulation of RA

A more complete understanding of the roles RA plays during development was built as scientists learned how to fully deprive embryos of RA. In parallel, exogenous RA and deletion of genes that degrade RA corroborated some of RA's developmental roles and revealed teratogenic effects of RA when concentrations reached levels that were significantly higher than what was physiologically observed. I will briefly summarize some of these effects because they illustrate the possible ways in which RA acts in regulation of the pectoral fin field.

Pregnant rodents were initially deprived of RA through a vitamin-A deficient (VAD) diet. This resulted in a range of malformations in tissues such as the eye, genital-urinary tract, heart, respiratory tract, and aortic arches [34], [35], [36]. Simultaneous loss of alpha and gamma RAR paralogs later recapitulated most of the VAD-associated congenital defects, revealing that there was redundancy between these paralogs [37], [38], [39]. The most severe defects associated with RA deficiency were revealed in the first RALDH2 mutant, which included an abnormal heart, an open neural tube, reduced otocysts, loss of brachial arches 2-3 and loss of forelimbs [40]. Importantly, the loss of forelimbs was not seen through prior RA deficiency approaches. This requirement for RA is conserved in formation of the zebrafish pectoral fins where Aldh1a2 mutants fail to develop pectoral fins [41], [42].

Simultaneous depletion of the three Cyp26 paralogs, Cyp26a, Cyp26b and Cyp26c revealed that they all contributed to regulation of RA in the zebrafish hindbrain [43]. A range of developmental phenotypes were observed such as exencephaly and posteriorizing of the rostral hindbrain [43], [44], [45], [46]. Importantly, these phenotypes corroborated the defects seen in RA deficient embryos suggesting that they reflect how RA normally behaves as opposed to reflecting artifacts that result from excess RA.

1.3.5 Instructive vs permissive roles for RA: The limb bud

Despite the clear phenotypes in RA deficient embryos, it is not clear whether RA plays an instructive role at discrete levels or if RA is a permissive signal that allow other signals to instruct development. In this section, I'll briefly highlight studies of the limb bud and the hindbrain where these conflicting models have been used to explain how patterning is regulated.

Morphologically distinct skeletal structures form along the PD axis of the forelimb,

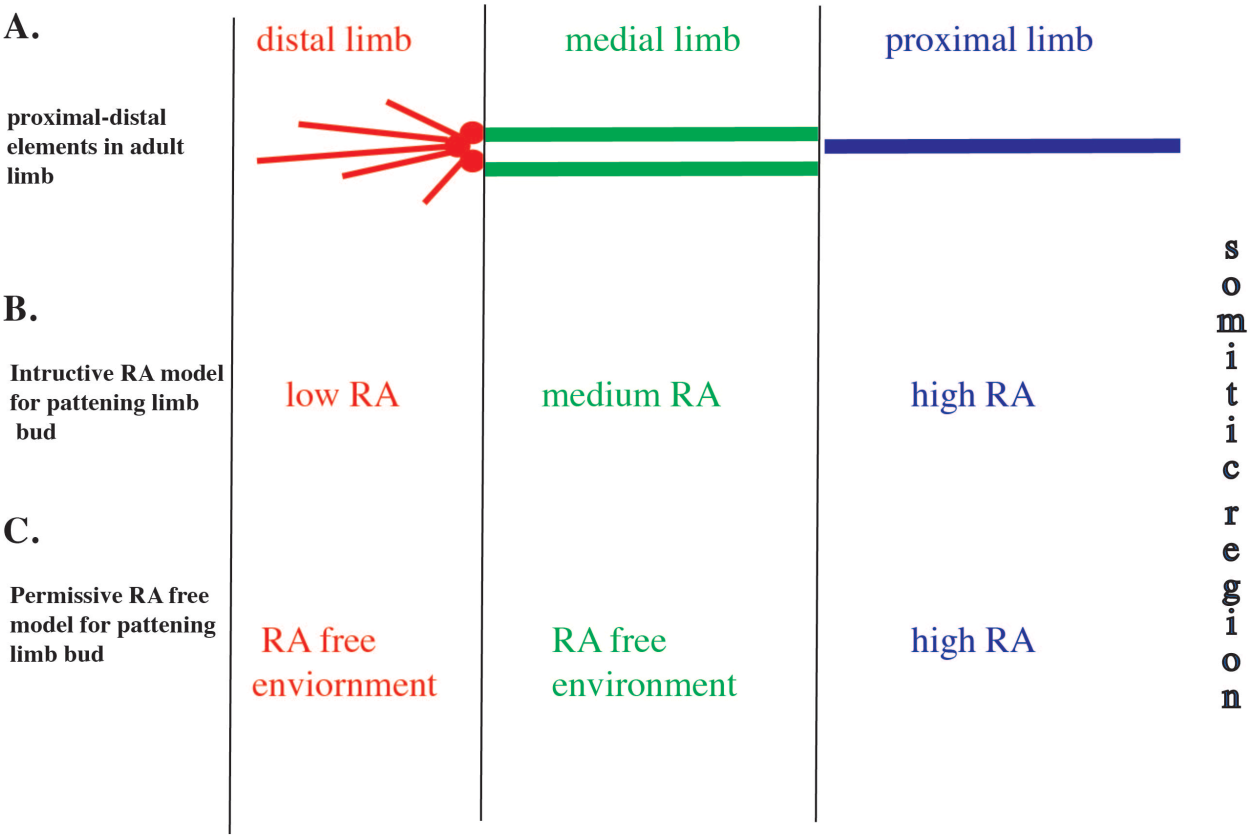

Fig.1.2 Instructive vs permissive roles for RA in patterning skeletal elements of the PD limb. (A) Illustration of skeletal elements of the limb bud beginning with the proximal stylopod (blue), followed by medial zeugopod(green) and distal autopod (red). (B) An instructive model for RA in specification of the PD skeletal elements suggests high levels of RA specify the stylopod, medium levels specify the zeugopod and low levels specify the autopod. (C) A passive model for RA suggests RA specifies the proximal region, but the clearance of RA in more distal regions of the limb bud is necessary for zeugopod and autopod elements to form.

beginning with the stylopod, followed by the zeugopod and autopod (Fig.1.2 A). Prior to formation of these skeletal elements, *MEIS1/2* genes are turned on in the proximal limb bud, *HOXA11* in the medial and *HOXD13* in the distal limb bud [47], [48], [49]. This patterns of gene expression is believed to specify the skeletal structures of the limb. In an instructive RA model, RA diffuses from the somitic region to form a gradient that is highest in the proximal limb bud and lowest in the distal limb bud. Here, discrete levels of RA establish the *MEIS, HOXA11* and

HOXD13 regions through into the limb bud region [50], [51], [52] (Fig.1.2 B). In a permissive RA free model, the medial and distal limb bud regions form in an environment that is free of RA (Fig.1.2 C). This implies there is a binary RA (proximal) and RA-free region (medial and distal) rather than a gradient of RA. In this model, RA has teratogenic effects in the medial/distal limb which means an RA free region is permissive and simply allows other signals to specify [53]. However, the existence of these RA-free regions have been difficult to confirm since direct ways to reliably visualize RA do not exist [54].

1.3.6 Instructive vs permissive roles for RA: The hindbrain

As in the limb bud, the hindbrain depends on careful regulation of RA to regulate patterns of gene expression and studies have also given rise to different models for how RA acts. In support of an instructive role for RA in patterning the hindbrain along the AP axis, different concentrations of a RA inhibitor were used to show that a gene expressed in rhombomere 8 needs to reach a higher threshold of RA compared to rhombomere 1. A low concentrations of RA inhibitor brings RA levels below the RA threshold for rhombomere 8 without affecting the other segments. Increased doses progressively affect more rostral rhombomeres [55], [56]. Increased concentrations of exogenous RA treatments were used to further corroborate these findings [53], [57].

A gradient free RA model for patterning the hindbrain assumes binary RA and RA-free zones are established rather than a gradient. The specific rhombomeres that express *cyp26* changes during development, supporting the idea RA is cleared from specific segments to allow rhombomere specific genes to turn on. This clearance of RA may then allow downstream factors such as Fgf or Wnts to specify rhombomere segments [41], [43], [56], [58].

1.4 The Cdx family of transcription factors

The Cdx transcription factors are implicated in regulation of the limb field in three ways. First, they regulate trunk *Hox* genes directly through modification of chromatin architecture [59]. Among these, HOX5 and HOX9 paralogs can directly bind a *Tbx5* enhancer in mouse. Secondly, Cdx paralogs have been implicated in direct regulation of *Tbx5*, a key gene expressed in the limb field [60]. Lastly, Cdx paralogs regulate gene expression associated with the RA pathway [61], [62]. Furthermore, Cdx transcription factors are good candidates in relation to control of *tbx5a* and the pectoral fin field along the body axis.

1.4.1 Cdx Transcription factors regulate development through control of transcription

The *cdx* genes are homologs of the Drosophila *caudal* gene [63], [64], [65], [66]. The main function of Cdx factors is to regulate gene expression by binding to cognate response element (CDRE) TTTATG to either activate or repress transcription [67], [68], [69], [13], [70], [71], [72]. The Cdx transcription factors also bind to members of the Swi/Snf chromatin complex such as Brg-1 to repress gene expression in gastrointestinal cells and in the yolk sac [60], [73], [74].

The Cdx factors act in different germ layers to regulate development and different models exist for which genes act downstream of Cdx. In the next three sections, I will briefly highlight some of the mechanisms by which Cdx are believed to act during development.

1.4.2 Cdx factors act indirectly on growth and patterning of mesoderm through hox genes

The paraxial mesoderm gives rise to an elaborate axial skeleton with distinguishable

segments. In mouse, all three Cdx paralogs are involved in establishing the normal pattern of axial segments as loss of these paralogs result in anterior homeotic transformations of cervical (C) or thoracic (T) vertebrae. These axial transformations correlate with posterior shifts in *Hoxc5*, *Hoxa7*, *Hoxb8* and *Hoxb9* expression in the paraxial mesoderm [75], [76]. Cdx binding sites have also been identified upstream of a number of these *hox* genes [77], [78], [79], [80], [81], [82]. Importantly, targeted deletion of *Hox* genes in mouse also results in similar homeotic transformations in the axial skeleton [80]. In Zebrafish, deficiency for Cdx4 or both Cdx4 and Cdx1a also results in posterior shifts in the expression of several *hox* genes in posterior mesoderm [81], [82], [83]. Cdx-deficient zebrafish embryos don't survive long enough to examine the axial skeleton but they fail to specify hematopoietic fates [81], [82]. Importantly, this defect can be rescued by overexpressing *hox8* or *hox9* genes. In addition to patterning, growth and elongation of axial progenitors in the tailbud region also depends on Cdx factors [81]. Mice and zebrafish embryos that are Cdx-deficient develop a severe truncation of the posterior region [84], [85], [86]. This elongation defect can also be rescued by ectopic *Hoxb8* or *Hoxa5* expression [87]. Together, all of these observations support a conserved role for *hox* genes downstream of Cdx in mesodermal growth and patterning.

1.4.3 Cdx factors act independently of hox genes in the neuroectoderm

The anterior neural plate gives rise to regions of the brain while the posterior region gives rise to the spinal cord. RA and Cdx are both necessary to properly form these territories along the AP axis. Studies support a mechanism where Cdx factors act independently of *hox* genes. *Cdx* genes are expressed in the spinal cord region where they directly repress hindbrain fate. Cdx-deficient embryos show loss of spinal cord genes and ectopic expression of hindbrain genes in

the spinal cord region [88]. Importantly, ectopic expression of *hox* genes does not rescue the repression of hindbrain as previously proposed in a separate study [89]. These studies suggest that Cdx factors act differently in the posterior neuroectoderm than the paraxial mesoderm.

In the more anterior region of the neuroectoderm nervous system where the spinal cord region transitions to hindbrain, RA and Cdx factors act antagonistically to determine where the transition forms. Loss of RA results in a rostral expansion of Cdx4 towards hindbrain region, suggesting RA acts upstream of *cdx* genes, similar to what was previously seen in mice [90]. [91]–[94]. Meanwhile, gain and loss of *cdx4* expression also results in changes in RA associated genes [55], [84], [90], [91], [94], [97]. Together, these studies support a complex model where Cdx factors act directly on spinal cord genes and through changes in RA to regulate development of the hindbrain and spinal cord.

1.4.4 CDX directly represses mouse Tbx5 expression

In mouse, CDX2 is believed to represses cardiac development independent of *hox* genes and RA. CDX2 directly binds numerous cardiac associated loci, that includes *Tbx5.* Foley and colleagues showed the *Tbx5* locus is normally enriched in CDX2 occupancy at two sites in mice during early development [60]. The expression of *Tbx5* was upregulated in the yolk sac of CDX1-/-, CDX2 -/- compound conditional null mice while hematopoietic genes were downregulated [81], [82], [97], [98]. This suggests CDX2 regulates mesodermal fates between blood and cardiac lineages in mice, in part, through *Tbx5* repression.

Cdx factors were also believed to repress cardiac development in zebrafish. Cdx1a and Cdx4 double deficient zebrafish show an up-regulation of *tbx5a* expression in the LPM [99]. In

this study, Cdx-deficient embryos formed a normal number of differentiating cardiac cells, but the authors still concluded that there was an expansion of pre-cardiac cells and there was no mention of pectoral fin development [99]. Overall, Cdx factors appear to have a conserved regulatory role for *Tbx5* in mouse and fish. However, there is no direct evidence to suggest this translates to an effect on cardiac development in zebrafish as seen in mice.

1.5 The Limb Field

Most of our understanding associated with the limb field has come from perturbations at pre-limb bud stages that later result in mis-placed or missing limbs. Studies associated with the limb field have also resulted in duplicated or ectopic limbs but these phenotypes resulted from concentrations of RA that were significantly higher than what is physiologically observed [100], [101], [102]. As a result, conclusions from these studies have been less reliable. The specific timing of perturbations that lead to ectopic or missing limbs is important because it reflects when the limb field is being specified in the embryo. Much of this work involved grafting experiments that were carried out in chick embryos [103]. Fate-map experiments that were performed in zebrafish have also revealed insight into when the pectoral fin field may be established [33], [104].

1.5.1 Formation of the limb field and Tbx5a

The T-box transcription factor *Tbx5* is the earliest marker for the limb field. *Tbx5* is specifically expressed in vertebrate forelimbs, while the related *Tbx4* gene is specifically seen in hindlimbs [105]. Each of these genes has a corresponding role in limb formation as embryos deficient in TBX5 never form forelimbs, while those deficient of TBX4 do not form hindlimbs

[106], [107], [108], [109], [110]. Expression of *Tbx4* and *Tbx5* first becomes visible in LPM much earlier than when the limb buds are initially visible. T-box genes were initially believed to be determinants of limb identity, where *Tbx5* specifically turned on in the forelimb field and *Tbx4* in the hindlimb field to specify limb identity [105], [111]. This role for T-box genes was later disproven in mice by showing TBX4 and TBX5 were interchangeable in promoting development of forelimbs [112].

Tbx5a is now generally accepted as a marker for the pectoral fin field in zebrafish. The pectoral fin was fate mapped to the region of the LPM where *tbx5a* is expressed at the 16 somite stage (16ss) [107], [113]. Loss of function studies also showed the individual cells that contribute to the fin bud require Tbx5a in order to migrate into the pectoral fin.

Classical embryological approaches revealed that the limb field in chick is established much earlier than when *TBX5* is first expressed in the LPM. The chick wing bud is first visible at Hamburger Hamilton stage 16 (HH16), while *Tbx5* is first expressed in the LPM at HH stage 14. Classical grafting experiments from the LPM of a donor as early as HH stage 8 (4 somites) of chick development induce an ectopic wing or leg in the coelom of a recipient embryo, depending on the region of the LPM the grafts originally came from [103]. High resolution lineage tracing of the LPM from the primitive streak stage showed that the limb, interlimb and hindlimb regions sequentially exit the primitive streak between stage 4 and 10 and that the limb region is specifically generated during HH stages 4 and 5 [114]. Together, these studies show gastrulation and early somitogenesis to be potential stages where the limb field forms [114].

Fate-maps done prior to induction of *tbx5a* in zebrafish suggest the pectoral fin field may be established during gastrulation. Pectoral fins have been roughly fate-mapped to a region of the gastrula called the lateral marginal zone (LMZ). Fate-mapping experiments between early (40%

epiboly) and late (85% epiboly) gastrulation in zebrafish embryos suggests the pectoral fin and nearby pharyngeal, blood and head vessel progenitors are formed during gastrulation along the classical dorsoventral (DV) axis, where a gradient of RA may already be established (Fig.1.1 C) [28], [115], [111].

1.5.2 RA and regulation of the limb field

The lack of forelimbs in RA deficient embryos is the result of failure to initiate *tbx5a* expression in the fin field region [10], [28], [92], [93], [94], [95], [120]. This was not immediately obvious because most RA deficiency studies prior to the first RALDH mutants were not severe enough to leads to loss of forelimbs (as mentioned in 1.2.4) [34], [34], [121], [122], [118]. RALDH2 mutants have a severe deficiency in RA that results in complete loss of *tbx5a* in the limb field [40], [120].

To address the developmental time in which RA signaling is required for the pectoral fins to form in zebrafish, researchers performed rescue experiments using Aldh1a2/Raldh2 mutants [42]. Exogenous RA treatments from 5hpf-13hpf (early gastrulation to 7ss) rescued pectoral fin development in RA deficient mutants. In a series of follow up studies, authors treated embryos with a reversible inhibitor of Raldh2 called DEAB to identify when formation of the fin field could be disrupted. This resulted in conflicted results where one group concluded RA was required prior to the tailbud stage (10hpf) and the other concluded RA acted after gastrulation [42], [118]. These diverging findings are believed to result from the excessive concentrations of DEAB that were used after gastrulation [118]. As a result, it is still unclear when RA is necessary to allow formation of the fin field.

In addition to the time RA is required for fin formation, there is disagreement on the

mechanism by which RA acts. Three downstream targets of RA have been proposed to mediate regulation of *tbx5a* and the limb field.

Studies in mice led to the identification of two full RAREs along with 2 half RAREs in a mouse limb enhancer for *Tbx5* [124]. However, a separate study used CRISPR to delete the RAREs which resulted in perfectly normal forelimbs. The zebrafish CNS12 enhancer that drives fin specific expression of *tbx5a* was also deleted in this study and resulted in normal fin buds [125]. The implications were that RA is not necessary to directly turn on *Tbx5* or that additional RAREs exist that act redundantly with the RARE that was deleted.

Studies in zebrafish and mice have led to an alternative model where RA acts permissively to allow the limb field to form. RA deficient mice and zebrafish have increased expression of *fgf8* which is associated with development of the heart field in the adjacent LPM [115], [116], [126]. *Fgf8* expression expands into the posterior LPM where *tbx5a* is normally expressed. When *fgf8* is ectopically expressed in zebrafish, heart field markers also expand into the pLPM at the apparent expense of the fin field specific *tbx5a* expression [127]. This suggests that Fgf8 clearance from the prospective fin field regions is necessary. Researchers identified a RARE upstream of FGF8 [119]. In addition, the transient loss of Fgf8 signaling can partially restore pectoral fin development in RA deficient embryos [53], [119], [127]. The conclusion of these studies was that RA directly represses *fgf8* expression to create a permissive zone where the limb field can form. The implications of these findings are that regulators other than RA promote formation of the fin field. Furthermore, if the pectoral fins in RA and Fgf double-deficient embryos still form in the correct location, other factors must act in parallel on the limb field to refine the AP position during development. Factors such as Wnt2ba are known to

promote *tbx5a* expression as well, but these appear to act downstream rather than in parallel to RA [128], [129].

1.5.3 *Hox genes and regulation of the limb field*

In a previous section (1.3.2), I introduced *Hox* genes as key regulators of segment identity in the axial skeleton [130], [131], [132], [133], [134], [135]. The cervical and thoracic segments are particularly intriguing because the tetrapod forelimb reliably forms at the transition between cervical and thoracic vertebrae (Fig.1.3) [136]. The implication is that a combination of *Hox* genes which influence cervical and thoracic identity may also specify forelimb position. However, this includes a long list of potential *Hox* genes. Paralogous groups 4-8 all promote cervical identity while paralogous groups 9-10 repress thoracic identity [80], [137], [138], [139], [135], [136], [142].

Hox5 genes in particular have been implicated in regulation of the limb field. *Hoxb5* mutants form limbs that are shifted rostrally [143], [144]. In addition, HOX5 protein can bind the limb enhancer for *Tbx5.* However, as discussed in section 1.4.2, this limb enhancer is not necessary for forelimb development. Follow up studies where all HOX5 paralogs were deleted did not report any forelimb position shifts, suggesting that *Hoxb5* is the only *Hox5* gene that can influence the AP position of the forelimb [145], [146], [147],. Furthermore, the pectoral fin position is not affected in zebrafish embryos deficient for individual *hox5* genes [115], [143].

Deletion of all HOX9 paralogs does not result in any forelimb position abnormalities in mice [146]. However, in chick, expression of a dominant negative version of *HOX9* (dnHOX9) coupled with overexpression of *HOXB4* in the flank region leads to a caudal shift of the forelimb [114]. These findings imply that HOX9 genes repress formation of the limb field in chick.

The lack of phenotypes in mice where all *Hox9* genes were deleted suggest that there are either species specific differences in the HOX paralogs that regulate the forelimb field or that several different paralogous groups should be examined together rather than focusing on just

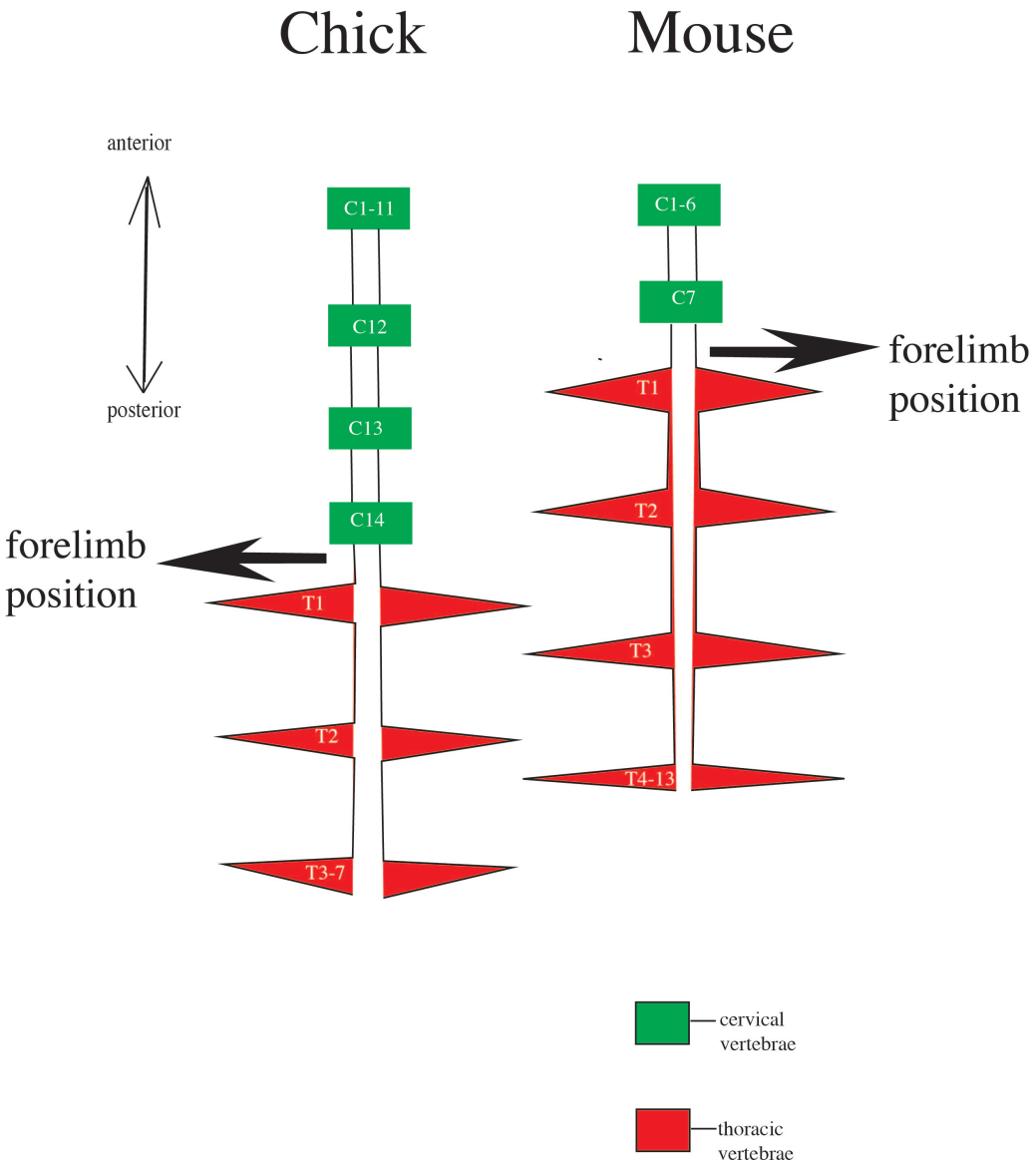

Fig.1.3 Position of the tetrapod forelimb correlates with where segments of the axial skeleton transition from cervical to thoracic identity. (A)The cervical segments of the chick axial column (green) transition to thoracic segments (red) at C14. The position of the forelimb (black arrow) is near the C14 -T1 transition. (B) The cervical segments (green rectangles) of the

Fig.1.3 (continued) mouse axial column transition to thoracic segments (red triangles) at C7. The position of the forelimb (black arrow) is shifted rostrally, compared to chick.

one group. Mis-regulation of factors upstream of *Hox* genes may provide an effective approach to learn more about how and when the limb field develops [51], [52], [147], [148], [144], [145].

1.6 Overview of Thesis

The developing forelimb has been a useful model for understanding morphogenesis and patterning. The mechanisms that drive these processes are critical to understanding how congenital limb defects arise. However, our understanding of how and when the limb field initially forms is limited. In chapter 3, I demonstrate that RA and Cdx1a/4 are critical for positioning of the limb field during gastrulation and that their mis-regulation leads to rostral or caudal shifts in position of the pectoral fin. The rostral fin shifts closely resemble congenital limb defects seen in humans such as Sprengel Deformity, where the arm and shoulder blade shift rostrally by 5-10cm. My hope is that the developmental time described in this thesis as well as the molecules will continue to be used by researchers to better understand how congenital limb defects arise.

CHAPTER 2

2. Materials and Method

2.1 Zebrafish Husbandry, heat shock and microinjection

Zebrafish were raised and maintained at 28.5° C in E3 media (5 mM NaCl, 0.17 mM KCL, 0.33 mM CaCl, 0.33 mM $MgSO_4$). Embryos were collected at the appropriate stage based on standards [151]. Embryos were collected from crosses between *AB stocks or from previously described transgenic zebrafish lines *Tg(tbx5a:eGFP*, [152] and (*Tg(h2afx:h2afv-mCherry)mw3* [153]. Heat shock-induced overexpression of *cdx4* was performed by moving *Tg[phsp70:cdx4]* embryos to a 39°C water bath for one hour.

2.2 Pharmacological treatments

The pan-Cyp26 inhibitor, Talarozole (also referred to as R1158866) was purchased from MedChem Express. The chemical was dissolved in dimethylsulfoxide (DMSO) to a stock concentration of 1mM and then diluted with 1X E3 media + 0.1%DMSO to a final working solution of 10uM and then stored at -20 degrees C for several months or at -80 degrees C for longer term storage. *AB or double transgenics were incubated in 1000ul working solution (~25 embryos with chorion) in glass vials in dark for 60 minutes beginning at either 4hpf (sphere), 7hpf (60% epiboly) or 11hpf (3ss). Following 60-minute treatments, embryos were rinsed 2-3x with 0.1% DMSO and then 2-3x in E3 media before being transferred to a petri dish where they were allowed to continue developing in E3 media.

2.3 In-situ hybridization and immunohistochemistry

Standard in-situ protocol using NBT/BCIP as the substrate was used for gene expression characterization of *aldh1a2* [41] *cdx4* (Skromne et al., 2007); *cyp26a1* [43] *dlx2a*; [154] *hoxd4a* [155]; and *no tail* [156]. Embryos were then rinsed and cleared with N-N-dimethylformamide (DMF) for 3hrs to overnight. Antibody stain was performed using mouse anti-myosin heavy chain at a concentration of 1:100 (A4.1025. Developmental Studies, Hybridoma bank, IA, USA). Anti-mouse IgG (H+L) secondary antibody (Vector laboratories, PI-2000) was used at 1:200 dilution. DAB color development was performed using the Peroxidase Substrate Kit (Vector laboratories, SK-4100).

2.4 Morpholino injections

Morpholino oligonucleotides against Cdx1a and Cdx4 were purchased from Gene Tools LLC with the following sequences:

anti-*cdx4* morpholino, 5'-CTCCAAAAGGTATCCAACGTACATG-3'

anti-*cdx1a*, 5'-CAGCAGATAGCTCACGGACATTTTC-3'.

Microinjection were performed at the 1 cell stage as previously described using standard protocol [88].

2.5 Imaging, cell tracking and statistical analysis

Images were collected on a Zeiss compound microscope using a Nikon-5000 camera and compiled using Adobe Illustrator. Measurements were performed using FIJI and statistical significance was determined using the student t-test (* indicates $p<0.05$, ** indicates $p<0.01$, *** indicates $P<0.001$, **** indicates $p<0.0001$). Live imagining was performed on a heated stage using dechorionated embryos mounted in 0.5% low melting-point agarose (Sigma;A9414) in E3

medium with 0.16% tricane. An upright Zeiss LSM710 confocal microscope with the Plan-Apochromat 20x/0.8 (working distance:0.5mm) objective was used to collect z-stacks every 8 minutes for 100 time points. Cell tracking was done on the first 50 time points using the Manual Tracking plugin for FIJI on. Further analysis was then performed by importing the tracking data to R. The following package was used to more consistently determine the somite level of origin https://github.com/erinboyleanderson/CellTrackingEBA

CHAPTER 3

THE CDX TRANSCRIPTION FACTORS AND RETINOIC ACID PLAY A PARALLEL ROLE IN ANTERO-POSTERIOR POSITIONING OF THE PECTORAL FIN FIELD

3.1 Abstract

The molecular regulators that determine the precise position of the vertebrate limb along the anterio-posterior axis have not been identified. One model suggests that a combination of *hox* genes in the lateral plate mesoderm (LPM) promotes formation of the limb field, but the redundancy among duplicated paralogs has made this model difficult to confirm. In this study, we identify an optimal window during mid-gastrulation stages when transient mis-regulation of retinoic acid signaling or the *caudal* related transcription factor, Cdx4, both known regulators of *hox* genes, can alter the position of the pectoral fin field. I show that increased levels of either RA or Cdx4 during mid-gastrulation is sufficient to rostrally shift the position of the pectoral fin field at the expense of surrounding gene expression in the anterior lateral plate mesoderm (aLPM). Alternatively, embryos deficient for both Cdx4 and Cdx1a (Cdx-deficient) form pectoral fins that are shifted towards the posterior and reveal an additional effect on size of the pectoral fin buds. Prior to formation of the pectoral fin buds, the fin field is visibly expanded into the posterior LPM (pLPM) region at the expense of surrounding gene expression. The effects on gene expression immediately post-gastrulation and during somitogenesis support a model where RA and Cdx4 act in parallel to regulate the position of the pectoral fin. My transient method is a potentially useful model for studying the mechanisms of limb positioning along the AP axis.

3.2 Introduction

There appear to be constraints in place for the ultimate position of forelimbs in tetrapods

as forelimb position corresponds to the vertebral region where cervical segments transition to thoracic segments. Earlier in development, when the developing forelimb is first visible as a limb bud, the limb bud position also appears to correlate with expression of *Hoxc6* in the somites [136]. In contrast, the expression of *hoxc6* in the zebrafish embryo does not exactly correspond with where the pectoral fin bud forms and other possible factors that regulate the position of the pectoral fins and the time of development are unknown. In addition, when these factors act to determine pectoral fin position is not known, although one likely possibility is that the time and position in which the progenitors of the pectoral fin initially form ultimately determines where the pectoral fin ends up.

Retinoic Acid (RA) signaling plays a role in induction and patterning of numerous organs during vertebrate development [18], [157]. In the Lateral Plate Mesoderm (LPM) of zebrafish, progenitors that give rise to blood vessels of the head are restricted by high levels of RA. RA also plays a role in limiting the number of cardiac progenitors, and complete loss of RA results in an expansion of cardiac associated genes into more posterior LPM (pLPM) [116]. Embryos deficient in Aldh1a2, the enzyme that synthesizes most of the embryonic RA, fail to form pectoral fins [41], [42]. In contrast, embryos deficient in Cyp26a, the primary RA degradation enzyme in the early embryo, have a prolonged increase in RA and later form defects in pectoral fin patterning, outgrowth and potentially in AP position [158]

The time of development in which RA may specifically regulate position of pectoral fin progenitors is unknown but long durations of RA deficiency specifically during gastrulation or somitogenesis via inhibitors of Aldh1a2, prevents pectoral fin progenitors from forming [117], [118]. During mid-late gastrulation, *aldh1a2* and *cyp26a* are in proximity to the lateral marginal region, the area fate mapped to give rise to pectoral fin [33], [104].

RA acts in part through activation of the t-box gene, *Tbx5,* which is the first gene to be expressed in the progenitor cells that later form the vertebrate forelimb [105], [159] Vertebrate embryos deficient for TBX5 fail to form forelimbs [106], [107], [110], [129]. TBX5 plays an essential role in the early initiation of the wing bud by promoting an epithelial to mesenchymal transition of the LPM in chick [160]. In zebrafish, Tbx5a directs the migration of the pectoral fin precursors into the prospective fin bud region [107], [113].

The Caudal (Cdx) transcription factors are key regulators of AP identity and axial elongation during vertebrate development [130]. Zebrafish have three Cdx paralogs, Cdx1a, Cdx1b and Cdx4, with Cdx1b mainly associated with phenotypes related to early endoderm formation [161]. *Cdx* genes in zebrafish and mouse directly bind to loci associated with factors of the RA signaling pathway such as *cyp26a* [60], [95], [96]. Loss of *cdx* genes in zebrafish and mouse results in mis expression of *cyp26a* and *aldh1a2*/*Raldh2* [62], [87], [89], [95], [162]. Patterning defects in the foregut, kidney and nervous system of Cdx-deficient embryos result in part from changes associated with RA signaling [61], [62], [163]

Cdx factors also bind directly to numerous loci associated with formation of cardiac and hematopoietic lineages [60], [96]. In particular, Cdx factors bind directly to *Tbx5* in mouse*,* and CDX-deficient mice ectopically express *Tbx5* and *Nkx2.5* in the yolk sac [60]. This ectopic expression appears to come at the expense of hematopoietic gene expression and suggest that in mouse, CDX regulates mesodermal fates between cardiac and hematopoietic lineages [60]. In zebrafish, Cdx-deficient embryos also ectopically express *tbx5a* [99]. However, the consequences of this expansion of *tbx5a* are unclear since Cdx-deficient embryos go on to form a normal number of differentiating cardiac cells [99] .

In this work, I determine that RA and the Cdx transcription factors play a related role in regulation of LPM derivatives such as the pectoral fin field. Increasing levels of RA or Cdx4 during gastrulation results in a rostral shift of the fin field. I also show that Cdx-deficiency leads to a caudal expansion of the fin field that later results in a pectoral fin bud that is increased in size and shifted posteriorly. By examining the early effects of RA and Cdx, I determine that Cdx and RA act in parallel pathways to restrict the AP position of the fin field.

3.3 Results

3.3.1 Increased levels of RA during gastrulation are sufficient to shift the pectoral fins rostrally

A combination of rostral fin shifts as well as delayed and shorted fin buds were previously reported in zebrafish with a nonsense mutation in the RA degradation enzyme, Cyp26a [158]. This presumably results in increased levels of RA at all stages of development. I first investigated whether increasing RA during a transient window by inhibition of Cyp26a was sufficient to induce changes in the AP position of the pectoral fin bud without resulting in delayed or shortened fin buds. *Cyp26a* is first expressed during gastrulation at the blastoderm margin and dorsal ectoderm at 4hpf. Additional Cyp26 paralogs (*cyp26b1 and cyp26c1)* are only expressed in segments of the hindbrain and not until after gastrulation [29], [43], [164], [165]. I inhibited Cyp26a activity by treating embryos with a pan Cyp26 inhibitor called Talarozole (also referred to as R115866) that was previously shown to phenocopy loss of Cyp26 activity in the zebrafish and mouse embryos [32], [43], [166]. I then characterized the AP position of the pectoral fin buds in Talarozole-treated embryos compared to controls at 36hpf. In DMSO-treated controls at 36hpf (Fig.3.1 A), the left pectoral fin bud forms at the level of somites 2-3 (somites are labeled brown and somite 3 is indicated) [167]. *Tbx5a* expression is used to visualize the

whole fin mesenchyme. In Talarozole-treated embryos, the fin buds are shifted rostral to somite 1 (Fig.3.1 B, somite 1 is indicated). Based on the expression of *tbx5a,* the pectoral fin is comparable in size with that of DMSO-treated controls. I then examined the AP polarity of these fin buds using *shh*, which is specifically expressed in the posterior fin mesenchyme. In DMSO-treated controls, *shh* is restricted to the posterior fin region, as expected (Fig.3.1 C). The expression of *dlx2a* is also shown, which marks the fin anterior ectodermal ridge (AER) and facilitates visualization of *shh,* relative to the whole fin bud. The pectoral fin buds in Talarozole-treated fish also express *shh* in the posterior fin mesenchyme. The area of expression is significantly expanded in these embryos, suggesting there is a patterning defect (Fig.3.1 D). A similar expansion of *shh* was previously reported in embryos exposed to excess RA [154], [158]. Expression of *dlx2a* was also upregulated in Talarozole-treated embryos.

I did not observe any obvious defects associated with somitogenesis. Related to this, a previous study showed that somitogenesis occurs normally in RA deficient zebrafish [168]. However, in Talarozole-treated fish, I did sometimes observe ectopic expression of Myosin anterior to the first somite that extended towards the shifted fin bud (Fig.3.1 D).

In order to identify when increased RA had the strongest effect on AP position of the pectoral fins, I examined the frequency of rostral fin shift that result from applying Talarozole to embryos for one hour beginning at either 4hpf, 7hpf or 11hpf (Fig.3.1 E, orange columns). These stages were selected randomly between the onset of *cyp26a* and the stage where the pectoral fin field is first visible by gene expression. Compared to DMSO-treated controls which all form pectoral fins at somite levels 2-3, embryos treated with Talarozole beginning at 4hpf results in a fin shift rostral to somite 1 in 90% of treated embryos (Fig.3.1 E). Compared to DMSO-treated controls at 7hpf, embryos treated with Talarozole at this stage also had a high frequency of

rostral fin shifts (35/38). Talarozole treatments that began at 11hpf resulted in a significant decline in the frequency of rostral fin shifts (3/20 embryos). In a small subset of fish, I also observed an asymmetry phenotype, where one fin bud was either reduced in size or missing, (Fig.3.1 E). From these findings I conclude that high levels of RA are sufficient to alter position of the pectoral fin bud during gastrulation. For the subsequent experiments in this work where I show Talarozole-treated embryos, I began treatment at 7hpf.

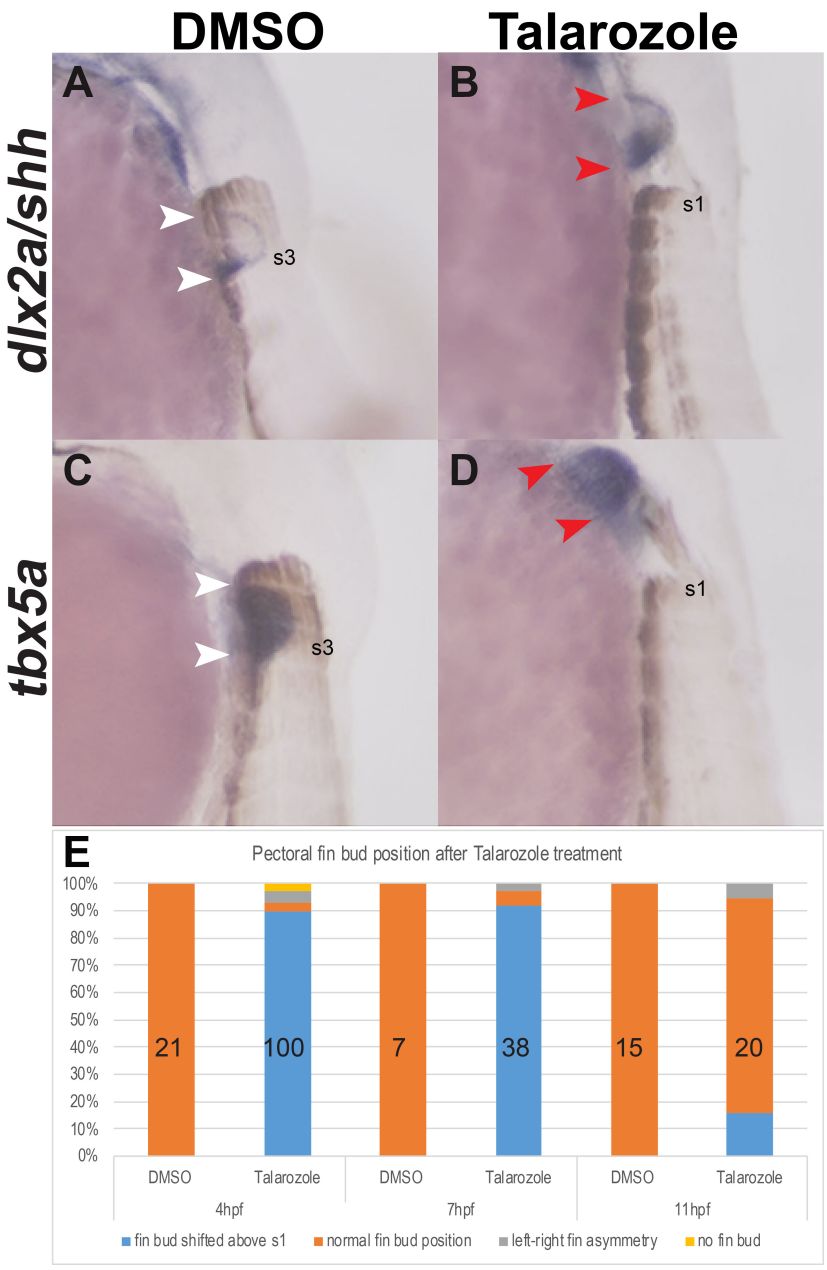

Fig.3.1 Increased levels of RA during gastrulation are sufficient to shift the pectoral fins rostrally. (A-D) In situ hybridization for the pectoral fin markers *dlx2a/shh* (A-B) and *tbx5a* (C-D) in lateral view at 36hpf show rostral fin shifts relative to the somites (brown). Fin bud forms at the level of somites 2-3 in DMSO-treated controls (white arrowheads in A, C). Pectoral fin buds form rostral to somite level 1 in Talarozole-treated embryos (red arrowheads B,D). Somites 1 or 3 are indicated (s1 and s3, respectively). (E) Quantification of the frequency of rostral fin shifts at 36 hpf after one hour of Talarozole application beginning at either 4, 7 or 11 hpf. Number of embryos examined are indicated in black.

3.3.2 Cdx1a and Cdx4 regulate the position of the pectoral fin buds along the AP axis

Cdx factors are known regulators of *hox* genes, which have been implicated in regulating limb position. Loss of *Hoxb5* results in a rostral forelimb shift in mice while mis-regulation of *HOX4/9* genes lead to caudal forelimb shifts in chick [114], [144]. To examine whether Cdx factors have an effect on pectoral fin development, I compared wild type embryos with double Cdx1a-deficient and Cdx4-deficient embryos (hereafter referred to as Cdx-deficient embryos) at 36hpf, when the larval pectoral fin buds are clearly visible. I visualized the somites using an antibody against myosin heavy chain (MHC) to establish the relative position of the pectoral fins. The fin buds normally form adjacent to the 2nd and 3rd somite. At this stage, as shown in wild type embryos in a lateral view of the left fin bud, the pectoral fins express *dlx2a* in the apical ectodermal ridge (AER) of the fin bud (Fig.3.2 A). To examine if AP polarity was established in the fin buds of these embryos, I co-stained for *shh*, whose expression is localized to the posterior fin mesenchyme. In Cdx-deficient embryos, *dlx2a* is noticeably upregulated in the fin AER, and expression is now observed adjacent to somites 3-7 (Fig.3.2 D). Expression of *shh* is still localized to the posterior fin mesenchyme, and also mildly upregulated, as seen adjacent to somites 6-7 (Fig.3.2 B). There is a subtle delay in the onset of *shh* expression as I do not detect expression in Cdx-deficient embryos at 32hpf, during which expression is clearly visible in wild type (data not shown). The expression of *tbx5a* was used to visualize the overall size of the fin buds. In Fig.3.2 E, *tbx5a* extends along the AP axis of the wild type fin bud, between somites 2-3, while in Cdx-deficient embryos, *tbx5a* expression begins between somites 3-4 and extends posteriorly to somite 7 (Fig.3.2 F).

To further demonstrate a role for Cdx factors on pectoral fin bud positioning, I transiently overexpressed *cdx4*. A prior mouse study showed increased levels of CDX1 resulted in reduced forelimbs [78], so I hypothesized that increased levels of Cdx4 would truncate or reduce the pectoral fin bud during a specific developmental window. I used *Tg[phsp70:cdx4]* fish previously described in (Skromne et al., 2007), to transiently induce *cdx4* expression throughout the embryo. Heat shock controls (HS controls) were *AB fish that were heat shocked during the same developmental time window as *Tg[phsp70:cdx4]* embryos. Compared to HS controls, which always formed fin buds at the normal position adjacent to somites 2-3 (Fig.3.2 I), induced overexpression of *cdx4* led to a high frequency of embryos that formed fin buds rostral to somite 1. In HS controls, *dlx2a* expression was localized in the AER adjacent to somites 2-3, and *shh* was restricted to the posterior fin mesenchyme adjacent to somite 3 in a pattern indistinguishable from wild type (Fig.3.2 C). In heat shocked induced *Tg[phsp70:cdx4]* embryos, *dlx2a* expression is visible in the AER but noticeably shifted anterior to the level of somite 1 (Fig.3.2 D). Normal fin polarity is established since *shh* is localized to the posterior fin mesenchyme. As indicated by the white arrowheads in Fig.3.2 E, HS controls have a normal level of *tbx5a* expression that runs adjacent to somites 2-3. In heat shock-induced *Tg[phsp70:cdx4]*, *tbx5a* expression is shifted rostral to the level of somite 1 but compared with HS controls, there is no visible effect on the overall size of the fin bud compared to HS controls (Fig.3.2 H).

In order to determine the optimal window where induced overexpression of *cdx4* results in the highest frequency of rostral fin shifts, I heat shocked *Tg[phsp70:cdx4]* embryos for 1hr beginning at 4hpf, 7hpf or 11hpf, prior to when the pectoral fin precursors begin to express *tbx5a.* I then examined the frequency of pectoral fin shifts at 36hpf. Heat shocked-induced overexpression of *cdx4* at 4hpf resulted in a moderate frequency (60%) of fin shifts rostral to

somite level 1 (Fig.3.2 I). The frequency of this phenotype peaked at 7hpf where I observed anterior fin shifts in 29/32 fish. At 11hpf, there was still a moderate frequency of rostral fin shifts (14/40) (Fig.3.2 I). In a subset of fish, I also observed an asymmetry phenotype, where one fin bud was either reduced in size or missing, (Fig.3.2 I, gray column). For all following experiments, unless stated otherwise, I induced *cdx4* overexpression at 7hpf when I observed the greatest frequency of rostral fin shifts while still maintaining relatively normal fin morphology.

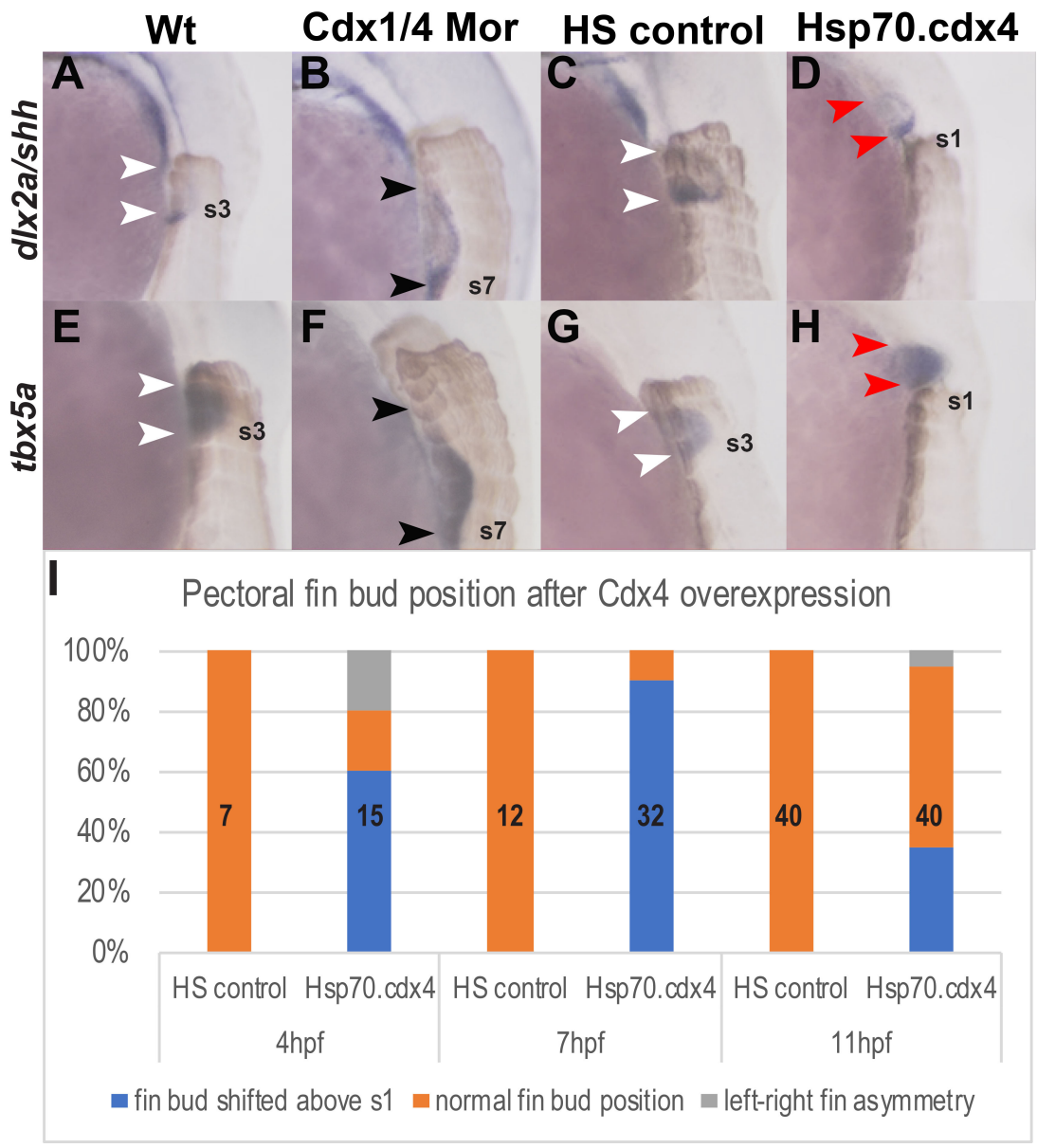

Fig.3.2 Cdx1a and Cdx4 regulate the position of the pectoral fin buds along the AP axis. (A-H) In situ hybridizations for the pectoral fin AER marker *dlx2a* (A-D), *shh* (A-D) and *tbx5a* (E-H) in lateral view at 36hpf show caudal shift and expansion of the fin buds (B,F) as well as rostral fin shifts of the pectoral fin (D,H) relative to the somites (brown). Fin buds are positioned at the level of somites 2-3 in wt (white arrowheads indicate somite level 3 ,A,E,). Pectoral fin buds from at somite level 3-7 in Cdx-deficient embryos (black arrowheads indicate somite level 7, B,F that form adjacent to somites 3 and somite 7 (indicated as s7). Pectoral fin buds form at somite levels 2-3 in HS controls (white arrowheads,C,G) while in Hsp70.cdx4 fish, they form rostral to the level of somite 1 (red arrowheads, D,H). (I) Quantification of the frequency of rostral fin shifts after induced cdx4 overexpression beginning at either 4,7 or 11hpf. Number of embryos used is indicated in black

3.3.3 Increased Cdx4 or RA results in mis-patterning in the aLPM

In order to examine whether Cdx4 and RA were having the same effect earlier in development, I compared gene expression in the aLPM in Talarozole-treated and heat-shocked induced *Tg[phsp70:cdx4]* embryos. I hypothesized that the rostral fin shifts resulted either from changes to where fin precursors were specified or changes to where they migrated after being specified. In the case of the former, I would expect a rostral shift of the fin precursors to affect the pattern of gene expression in the aLPM. The aLPM contains myocardial, pharyngeal and vascular progenitors, which were previously shown to be sensitive to increased levels of RA [116], [162], [169]. During gastrulation, *cdx4* is expressed near the lateral marginal zone (LMZ) associated with the fate-mapped location of pectoral fin, blood, and cardiac precursors [33], [82], [104], [116]. After gastrulation, *cdx4* expression has regressed away from the aLPM, towards the tailbud. At 14hpf as shown in a dorsal view with the anterior end oriented towards the top, in HS controls, the stem cell leukemia gene, *scl-1*, begins to be expressed at the anterior end of the aLPM. Expression of *scl-1* was previously fate mapped to cranial vasculature [169]. Expression of this gene extends caudally down the embryo as two bilateral stripes with a posterior boundary just above the level of the anterior end of the notochord (Fig.3.3 A). In heat-shocked induced *Tg[phsp70:cdx4]* embryos, *scl-1* expression is observed with an anterior boundary that is similar to HS controls but is noticeably truncated in length at the posterior end (Fig.3.3 B). Talarozole treatments lead to a similar result at 14hpf as that observed in heat-shocked induced *Tg[phsp70:cdx4]* embryos. In DMSO-treated controls, the overall length of *scl-1* expression is localized to the aLPM in a similar pattern to HS controls (compare Fig.3.3 C with Fig.3.3 A), while in Talarozole-treated embryos, the length of *scl-1* is severely truncated at the posterior end (Fig.3.3 D), resembling the effect seen in heat-shocked induced *Tg[phsp70:cdx4]* embryos

(Fig.3.3 B).

To compare the effect of increased RA and Cdx4 on gene expression posterior to *scl-1,* I examined the anterior boundary of *tbx5a* and *hand2* expression, which corresponds to the aLPM where cardiac precursors reside at this stage [170]. In HS controls, I observe a noticeable gap between the rostral boundary of *tbx5a* expression in the LPM and the eye (Fig.3.3 E). This distance is significantly reduced in heat-shocked induced *Tg[phsp70:cdx4]* embryos, as the anterior limit of *tbx5a* in the LPM shifts rostrally towards the level of the eye (Fig.3.3 F). In DMSO-treated embryos, there is also a visible gap between *tbx5a* expression in the LPM and eye, while in Talarozole-treated embryos, there is a large rostral shift in expression of *tbx5a* towards the eye, indicated by the red arrowhead (Fig.3.3 G-H).

Cyp26 deficient embryos were previously shown to have a rostral shift in *hand2* expression in the aLPM, suggesting increased RA promotes this shift. I examined the effects of increased Cdx4 on *hand2* expression at the same stage. Expression of *hand2* in the aLPM extends bilaterally along the AP axis similar to *tbx5a.* In HS controls, the rostral boundary of *hand2* expression relative to the head is not noticeably different from that of heat-shocked induced *Tg[phsp70:cdx4]* embryos (Fig.3.3 I-J). In DMSO-treated embryos I did not observe a noticeable effect on *hand2* expression compared to HS controls, however there is a sizable rostral shift of *hand2* expression in Talarozole-treated embryos (red arrowhead in Fig.3.3 L) relative to DMSO-control embryos.

I quantified the AP length of *scl-1* and *tbx5a* expression under the above described conditions. In Fig.3.3 Q I normalized the length of *scl-1* expression to the trunk width and show that there was a statistically significant reduction in the *scl-1* length between HS controls and heat-shocked induced *Tg[phsp70:cdx4]* embryos (p value<0.001) as well as between DMSO and

Talarozole-treated embryos (p value<0.0001). I also quantified the shift of *tbx5a* expression relative to the posterior edge of the staining in the eye, as shown in Fig.3.3 R. The distance between the LPM and eye staining is significantly reduced between HS controls and heat-shocked induced *Tg[phsp70:cdx4]* embryos (p value<0.05) as well as between DMSO and Talarozole-treated embryos (p value<0.0001).

In order to specifically examine the pectoral fin precursors, I characterized expression of *tbx5a* in the pLPM at 18hpf. Initially, *tbx5a* is expressed as a continuous stripe within the LPM, where it marks fin and other progenitors. At 15ss, the LPM that expresses *tbx5a* separates to form anterior and posterior halves [107], [159]. By 18hpf, the anterior half has migrated rostrally and the posterior half now flanks somites1-4. This posterior half corresponds to the pectoral fin precursors [113], [171]. I examined the posterior expression of *tbx5a* at 18hpf, by counterstaining for the position of the somites using an antibody for Myosin Heavy Chain protein. As shown in (Fig.3.3 M), in HS controls, *tbx5a* expression is observed just rostral to the level of somite 1 and extends caudally, just below the level of somite 4. This matches the expression pattern I observe in wild type embryos (Fig.3.4 F). In heat-shocked induced *Tg[phsp70:cdx4]* embryos, the expression of *tbx5a* is shifted rostrally, with the posterior boundary now positioned adjacent to the level of somite 1 (Fig.3.3 N). DMSO-treated controls also show a wild type pattern of expression where *tbx5a* flanks somites 1-4 (Fig.3.3 O). Meanwhile, Talarozole-treated embryos also display a rostral shift in *tbx5a* and *hand2* expression, where the posterior boundary of expression is at the level of somites 1-2 (Fig.3.3 P). Taken together, these findings show that increased Cdx4 or RA each result in rostral shifts in *tbx5a* expression relative to both the eye and somites as well as a reduction in length of *scl-1* expression in the adjacent aLPM.

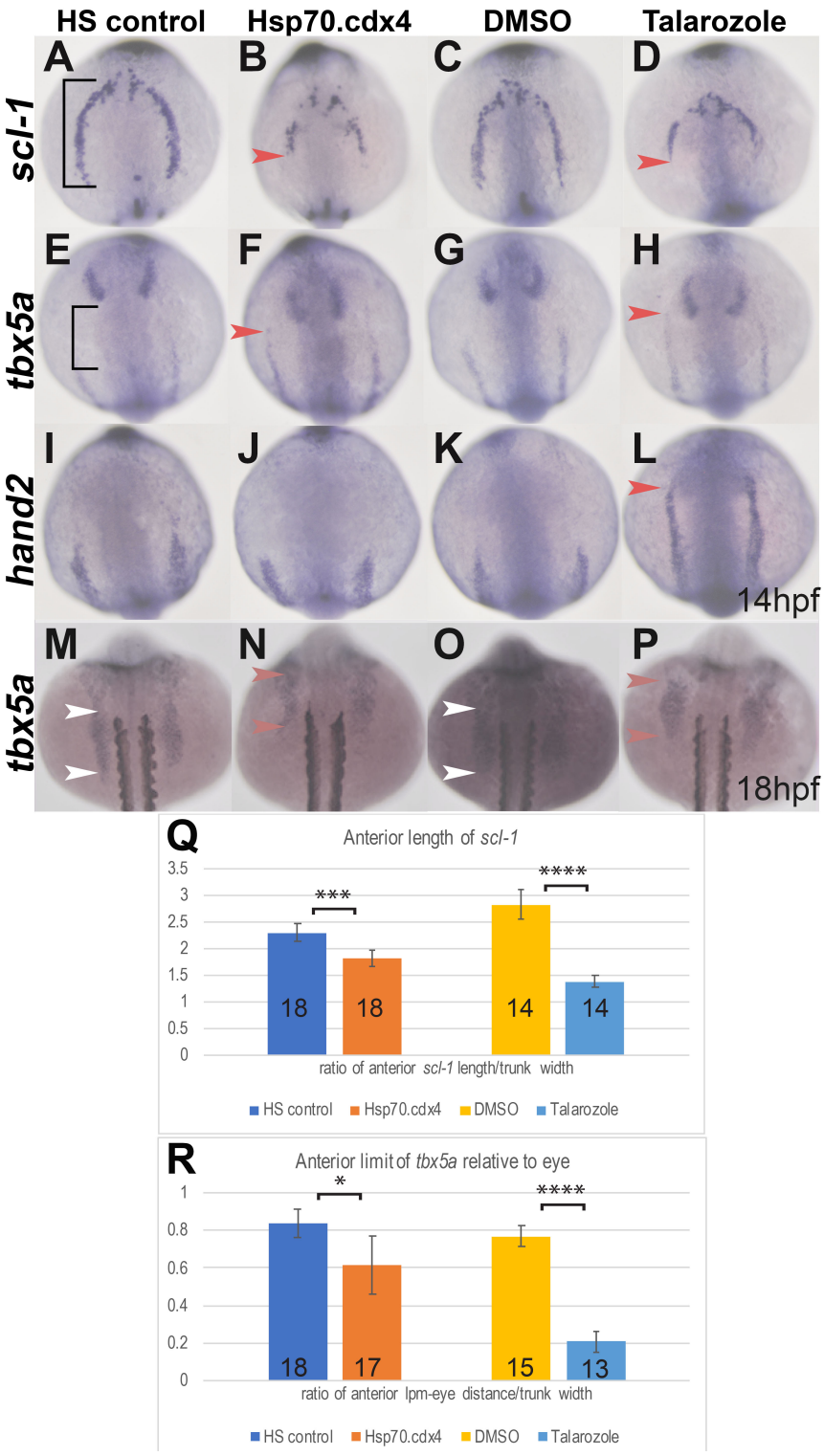

Fig.3.3 Increased RA or Cdx4 results in mis-patterning in the aLPM. (A-L) In situ hybridization at 14hpf for aLPM markers *scl-1* (A-D), *tbx5a* (F-I), and *hand2* (I-L) in dorsal view. The AP length of *scl-1* expression in HS controls (black bracket, A) is truncated in length

Fig.3.3 (continued) in Hsp70.cdx4 (B). Compared to the expression length of *scl-1* in DMSO controls (C) *scl-1* expression is also truncated in Talarozole-treated embryos (red arrowhead, D). The anterior boundary of *tbx5a* in the aLPM relative to expression in the eye (black bracket, E) is shifted rostrally in Hsp70.cdx4 (red arrowhead, E), compared to HS controls (E). Expression of *tbx5a* in the aLPM of Talarozole-treated embryos (red arrowhead, H) is also shifted rostrally, compared to DMSO-treated controls (G). The anterior boundary of *hand2* in the aLPM is unaffected between HS controls and Hsp.70.cdx4 (I,J). Expression of *hand2* shifts rostrally in Talarozole-treated fish (red arrowhead, L) compared to DMSO-treated controls (K). Expression of *tbx5a* in the pLPM at 18hpf is shifted rostrally in Hsp70.cdx4 embryos (red arrowhead, N) compared to HS controls (white arrowheads, M). Expression of *tbx5a* is also shifted rostrally in Talarozole-treated fish (red arrowhead, P) compared to DMSO-treated controls (white arrowheads, O). (Q) Quantification of the AP length of *scl-1* in the aLPM normalized the trunk width (brackets in A). (R) The rostral shift of *tbx5a* shown as length between the aLPM-eye (bracket, E), normalized to the width of the trunk. Statistical significance was determined using the student t-test (*, $p<.05$, ***, $p<.001$, ****$P<.0001$.

3.3.4 Cdx-deficient embryos have patterning defects in the pLPM

I was interested in examining whether the caudal shift or the expanded size of the pectoral fin in Cdx-deficient embryos (Fig.3.2 B,F) were also associated with patterning defects in the LPM. To facilitate this, I first compared gene expression in the aLPM as I did in Fig.3.3. In wild type, *scl-1* expression begins in the LPM near the head region and extends towards the posterior (Fig.3.4 A). In Cdx-deficient embryos, *scl-1* expression is located more medially and is disordered. However, the overall length along the AP axis is comparable with wild type embryos (Fig.3.4 B). I quantified the length of *scl-1* (as in Fig.3.3 Q) and observed a non-significant difference (NS) in length between wild type and Cdx-deficient embryos (p value>.05) (Fig.3.4 C).

I also examined the anterior boundary of *tbx5a* in the aLPM relative to the eye. The distance between *tbx5a* expression in posterior eye and the aLPM of wild type (bracket in Fig.3.4 D) wat not visibly different from that of Cdx-deficient embryos (Fig.3.4 D-E). I quantified this distance and saw no significant difference between wild type and Cdx-deficient embryos (p-value>.05, NS).

Previously, the pLPM at the level of somite 5 that is posterior to the expression of *tbx5a*, was fate-mapped to the peritoneum [113]. This region of the LPM expresses *hand2,* which partially overlaps with *tbx5a* and extends further posterior in the LPM. I examined *hand2* expression in the pLPM. In wild type embryos that are oriented laterally, *hand2* expression extends along the posterior LPM towards the tailbud region (Fig.3.4 G). In Cdx-deficient embryos, *hand2* expression is noticeably reduced in length to a faint area of expression near the tailbud region (Fig.3.4 H).

To specifically examine the AP position of the fin field, I compared expression of *tbx5a*

in the LPM between wild type and Cdx-deficient embryos at 18hpf. In wild type embryos, *tbx5a* expression extends from the level just rostral to somite 1 to the level of somite 4 (white arrowheads, Fig.3.4 K). In Cdx-deficient fish, the anterior limit of *tbx5a* begins rostral to the level of somite 1, similar to wild type. The posterior boundary is caudally expanded to the level of somite 7-8 (black arrowheads, Fig.3.4 L).

Between 18-24hpf, the Tbx5a-positive cells of the fin field converge along the AP axis to where the pectoral fin bud eventually forms. This convergence process requires an Fgf24 signal in order to direct the migration of these fin progenitors into the pectoral fin bud [113], [172]. To characterize convergence, I compared expression of *fgf24* between wild type and Cdx-deficient embryos at 18hpf. In wild type, I observe expression at the level of somites 2-3 (Fig.3.4 K). In Cdx-deficient fish, expression also begins at somite level 2 and extends posteriorly to somite level 4. Overall, the pattern of gene expression in the pLPM is altered in Cdx-deficient embryos.

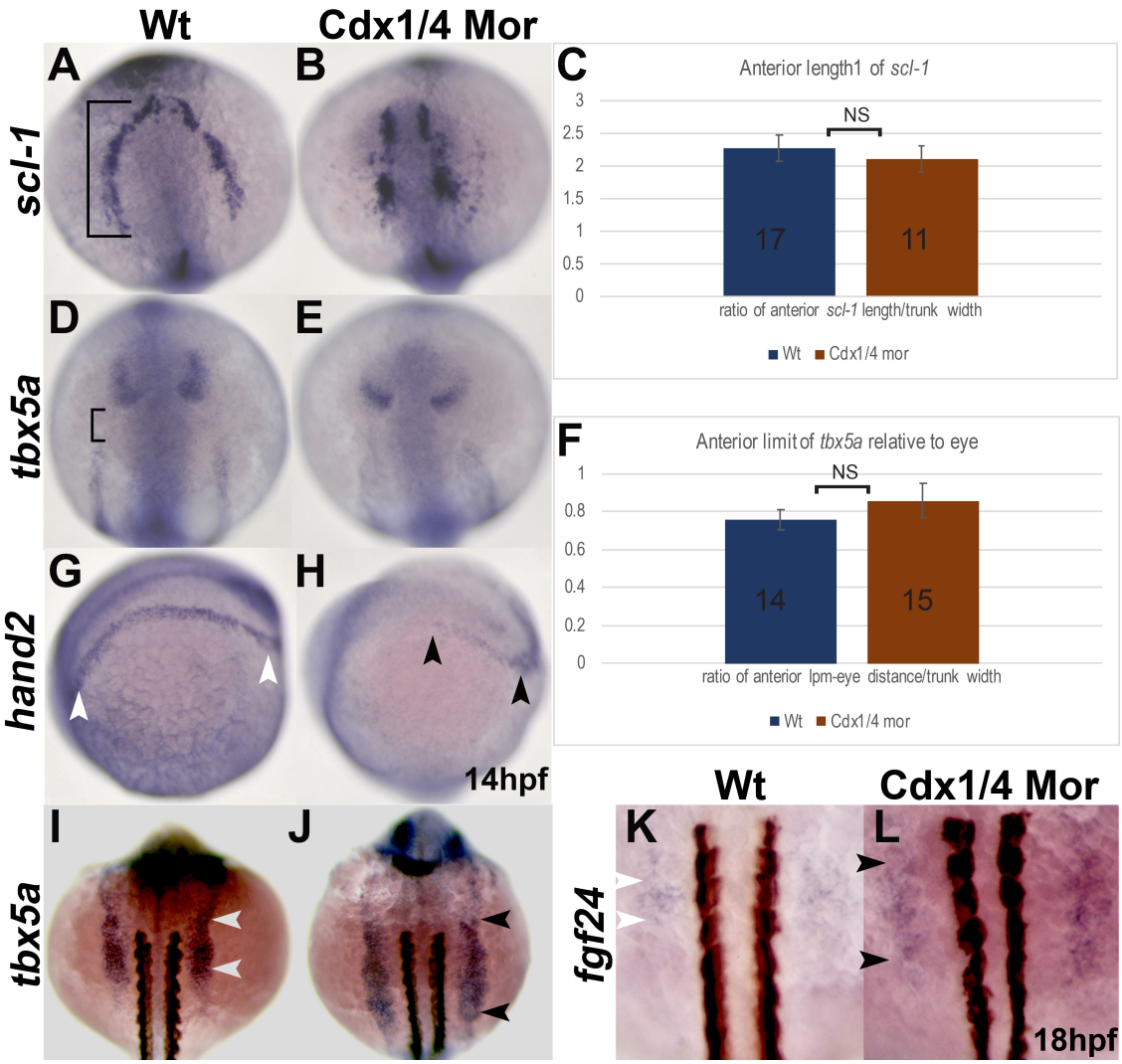

Fig.3.4 Cdx-deficient embryos have patterning defects in the pLPM. In situ hybridizations for *scl-1*(A,B) *tbx5a* (D-E) and *hand2* (G,H) at 14hpf as well as *tbx5a* (I-J) and *fgf24* (K,L) at 18hpf. (A,B) Wt and Cdx-deficient embryos are comparable in the AP length of *scl-1*. (C) Quantification of the AP length of *scl-1* (black bracket, A) normalized to the trunk width for wt and Cdx-deficient embryos. Expression of *tbx5a* relative to the eye is unaffected between wt and Cdx-deficient embryos (D,E). (F) Quantification of the AP length between *tbx5a* in the aLPM and the eye (black arrowhead, D) shown as a ratio of the distance between the aLPM and the anterior eye, normalized to the width of the trunk is comparable between wt and Cdx-deficient embryos. (G,H) The expression length of *hand2* in the pLPM is reduced in Cdx-deficient embryos (black arrowheads, H) compared to expression in wt (white arrowheads, G). (I,J) Expression of *tbx5a* at 18hpf is expanded posteriorly in the pLPM of Cdx-deficient embryos (black arrowheads, J), compared to wt (white arrowheads, I). (K,L) Expression of *fgf24* at 18hpf is expanded along the AP axis in Cdx-deficient embryos to somite levels 2-4 (black arrowheads, L) compared to wt where *fgf24* is expressed at the level somites 2-3 (white arrowheads, L).

Fig.3.4 (continued) Embryos are oriented in a dorsal view (A-B, D-E, I-L) or laterally with the anterior end towards the left (G-H). Non-significant differences in the quantitative analysis are indicated NS.

3.*3.5 A sub-population of Tbx5a-positive cells fails to migrate from the pLPM to the pectoral fin bud in Cdx-deficient embryos*

To confirm whether changes to *tbx5a* expression in Talarozole-treated embryos reflected changes in the population of cells that migrate into the fin bud region, I characterized the actual population of cells that migrate into the pectoral fin bud by backtracking the movements from time lapse videos of cells that originated from the anterior and posterior ends of the fin bud at 24hpf to the location in the LPM from which they originated at 18hpf. For these experiments, *Tg(tbx5a:eGFP)* fish, which were previously shown to recapitulate endogenous *tbx5a* expression were crossed to *Tg(h2afx:h2afv-mCherry)mw3* fish to allow me to observe the movements of the nuclei of *tbx5a* expressing cells. In Fig.3.5, the left sides of double transgenic embryos are shown as maximum intensity projections (MIP) post migration at 24hpf (Fig.3.5 A-H) and at the onset of migration around 18hpf (Fig.3.5 I-L). Tbx5a-positive cells that migrated into the fin bud by 24hpf are shown in (Fig3.5 A-D) and the nuclei of these cells are shown in (Fig.3.5 E-L).

In DMSO-treated controls, I backtracked 47 cells within the fin bud to the LPM between somite levels 1-4. In addition, a small fraction was observed to have derived from the region rostral to the first somite (Fig.3.5, J). In Talarozole-treated embryos, the entire fin bud region was located rostral to somite 1 (Fig.3.5 D,H) and of the backtracked 58 cells, 50 of these cells originated from the 18 hpf LPM rostral to somite 1, while 8 cells migrated from the level of somite 1. Cells from the LPM at somite levels 2-4, which did not express *tbx5a* (Fig.3.3 P) in Talarozole-treated embryos, never migrated into the fin bud region (Fig.3.5 J). These results

show that in Talarozole-treated fish, the region of the embryo with *tbx5a* expressing cells at 18hpf accurately reflected the population of cells that migrated to the pectoral fin bud.

In wild type embryos, the expression of *tbx5a* in the LPM is a reliable marker for the fin field at 18hpf. However, Cdx-deficient embryos have a significant expansion of *tbx5a* expression in the pLPM that in a previous study was reported to result from additional pre-cardiac cells. As a result, it is not clear whether these cells are true fin progenitors. To address whether these ectopic *tbx5a* expressing cells became cardiac or fin field cells, I again backtracked the movements of cells from both the anterior and posterior ends of the fin bud at 24hpf to their positions in the 18hpf LPM. In control embryos, six cells were back-tracked from the fin bud region to the LPM region rostral to the first somite, and 38 cells were back-tracked from the fin bud region to the LPM between the level of somites 1-4, (Fig.3.5 I). In Cdx-deficient embryos, cells rostral to somite 1 were never observed to contribute to the pectoral fin bud. In these Cdx-deficient embryos, 53 cells were back-tracked from the fin bud to the LPM between somites 1-6; within these embryos, 22 of these fin bud cells were shown to have derived from somite levels 5 and 6 (Fig.3.5 I,). In contrast, the *tbx5a*-positive cells from somite levels 7-8 were never observed to contribute to the pectoral fin bud despite the increased expression of *tbx5a* in the LPM at the level of somite 7-8 in these Cdx-deficient embryos. Therefore, the extent to which the fin field actually expanded is unclear and it is possible the expression of *tbx5a* in the LPM at 18hpf (Fig.3.4 H) no longer reflects the fin field in this background.

Although a subset of the Tbx5a-positive cells at 18hpf did not contribute to the fin bud region in Cdx-deficient embryos, the fin bud region was still visibly larger in diameter compared to controls at 24hpf. This difference was quantified by measuring the AP length of the formed fin bud region (Fig.3.5 K). The average length of the fin bud region in control embryos was 98.3um

while in Cdx-deficient embryos the average length was increased to 194.9um (p value<.01). Meanwhile, the average length of the fin bud region in DMSO-treated embryos was 91.8um comparable to the average length in Talarozole-treated embryos (99.3um(p value>.05, indicated NS).

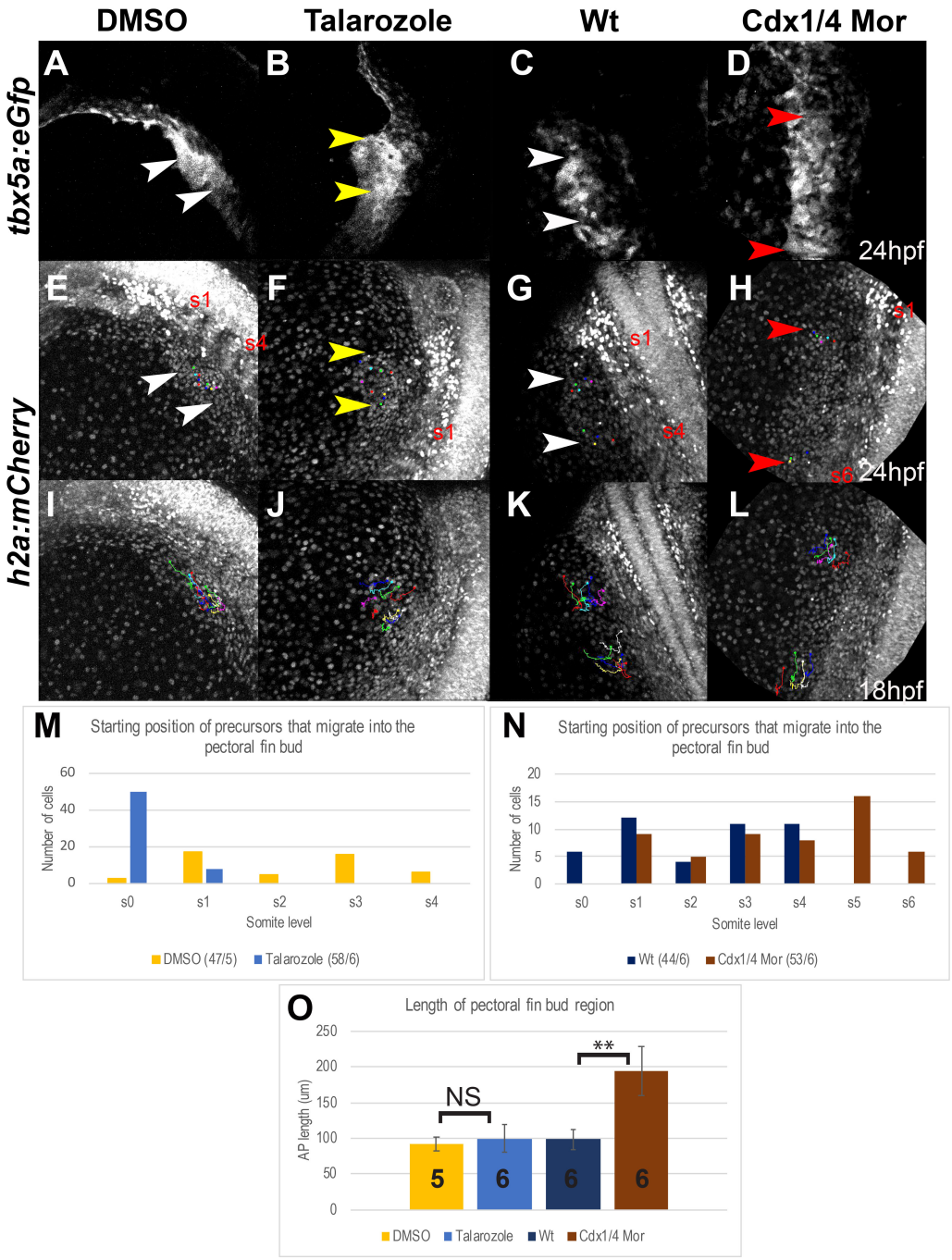

Fig.3.5 A subpopulation of Tbx5a-positive cells fails to migrate from the pLPM to the pectoral fin bud in Cdx-deficient embryos. (A-L) Maximum Intensity Projections (MIPs) of time lapsed *Tg(tbx5a:eGFP), Tg(h2afx:h2afv-mCherry)mw3* double transgenic embryos, oriented dorsally. The fin field cells that completed migration into the fin bud region are indicated by the arrowheads in *Tg(tbx5a:eGFP)* (A-D) and *Tg(h2afx:h2afv-mCherry)mw3* (E-H) embryos at 24hpf. Cells that were backtracked beginning at 24hpf are indicated by the colored

Fig.3.5 (continued) dots (E-H). The tracks for the selected cells are indicated by colored lines in *Tg(h2afx:h2afv-mCherry)mw3* embryos at 18hpf (I-L). The fin bud region at 24hpf is shown for wt (white arrowhead, A,E), Cdx-deficient (red arrowheads, B,F), DMSO-treated (white arrowheads, C, G), and Talarozole-treated (yellow arrowhead, D, H). The somite level of the anterior or posterior fin bud region is indicated (either S1 and S4 or S1 and S6). The somite level that Tbx5a-positive cells of the fin bud originated from at 18hpf are quantified for DMSO and Talarozole-treated embryos (M) or for wt and Cdx-deficient embryos (N). The number of cells tracked/the number of embryos used is indicated per condition as a fraction at the bottom of tables M-N. (O) Quantification of the length of the fin bud region at 28hpf for wt (navy blue), Cdx-deficient (brown), DMSO (yellow) and Talarozole (blue). Statistical significance was determined using the student t-test (**, $p<.01$) Non-significant differences are indicated NS.

3.3.6 Transient increases in Cdx4 or RA have different effects on gene expression at the tailbud stage

Similarities in the phenotypes that result from increased levels of Cdx4 or RA can be due either to these molecules acting in parallel or through one another to regulate the pectoral fin field. Prior studies have shown RA and Cdx can interact in distinct developmental contexts [61], [62], [89], [90], [99], [162]. To distinguish between these possible scenarios, I compared the transcriptional effects between heat-shocked induced *Tg[phsp70:cdx4]* and increased RA (via Talarozole treatments).

At the tailbud stage (10hpf), I compared expression of RA associated genes, namely *aldh1a2* and *cyp26a* which are both known to respond to changes in RA to mediate feedback responses [26], [28]. I also examined *hoxd4a* which shows a similar expression pattern to *cyp26a*, directly adjacent to *aldh1a2.* Interestingly, in a prior study, pectoral fins were fate mapped to the region adjacent to *aldh1a2* [33]. I therefore hypothesized potential changes at the anterior boundary of *aldh1a2* or the genes expressed anteriorly.

As shown in HS controls, a gap between the anterior *aldh1a2* and *ntl* expression boundaries (Fig.3.6 A) is present that is comparable to that of wild type (Fig.3.7 A). This gap is reduced in *Tg[phsp70:cdx4]* heat-shocked embryos (Fig.3.6 B). I quantified the *aldh1a2* shifts relative to the *ntl* expression and normalized these measurements relative to the diameter of the yolk. As shown in Fig.3.6 M, this reduction was highly significant (p-value<.0001) and appears to result from a rostral shift of the boundary of *aldh1a2* relative to *ntl* (Fig.3.6 A-B).

In DMSO-control embryos, the *aldh1a2* boundary is located in a similar position to HS controls (compare Fig.3.6 A, C), while in Talarozole-treated fish, the *aldh1a2* expression boundary is shifted caudally, relative to *ntl* (Fig.3.7 D). These measurements are quantitated in

(Fig.3.6 M) which shows a small, but significant change in this value for Talarozole-treated embryos.

While Cyp26a is key to regulation of RA levels, the *cyp26a* gene is also a very responsive downstream RA target. Changes to RA levels lead to differences in *cyp26a* expression. I examined the AP position of *cyp26a* expression in the trunk mesoderm, relative to the posterior boundary of *cyp26a* expression in the neural ectoderm. In HS controls, I observed a visible gap in expression between these regions (Fig.3.6 E). In heat-shocked induced *Tg[phsp70:cdx4]* embryos, I observed the same *cyp26a* expression pattern (Fig.3.6 E-F). I quantified the length between *cyp26a* in the trunk mesoderm and neuroectoderm, normalized to the diameter of the yolk, and saw no statistically significant difference (p-value>.05 in Fig.3.6 N). I also observed that compared to DMSO-treated controls, the expression of *cyp26a* in trunk mesoderm shifts rostrally towards the neuroectoderm in Talarozole-treated embryos (Fig.3.6 H). The distance between *cyp26a* expression in the trunk mesoderm and neuroectoderm is significantly reduced, as shown in Fig.3.6 N (P-value<.0001). Together, these results show that increased levels of Cdx4 affects the pattern of RA-responsive genes differently than increased levels of RA.

Hoxd4a expression initiates just after 10hpf, rostral to where *aldh1a2* is expressed [56], [173]. In HS controls there is a gap between the anterior *hoxd4a* expression limit relative to the anterior tip of the notochord (Fig.3.6 I). In heat-shocked induced *Tg[phsp70:cdx4]* embryos, *hoxd4a* shifts rostrally, closer to the end of the notochord (Fig.3.6 J). I observe a similar rostral shift in *hoxd4a* expression when I compare expression DMSO and Talarozole-treated embryos (Fig.3.6 L). These results are consistent with previous findings that show *hoxd4a* is mis-expressed due to changes in either RA or cdx4 [56], [83] .

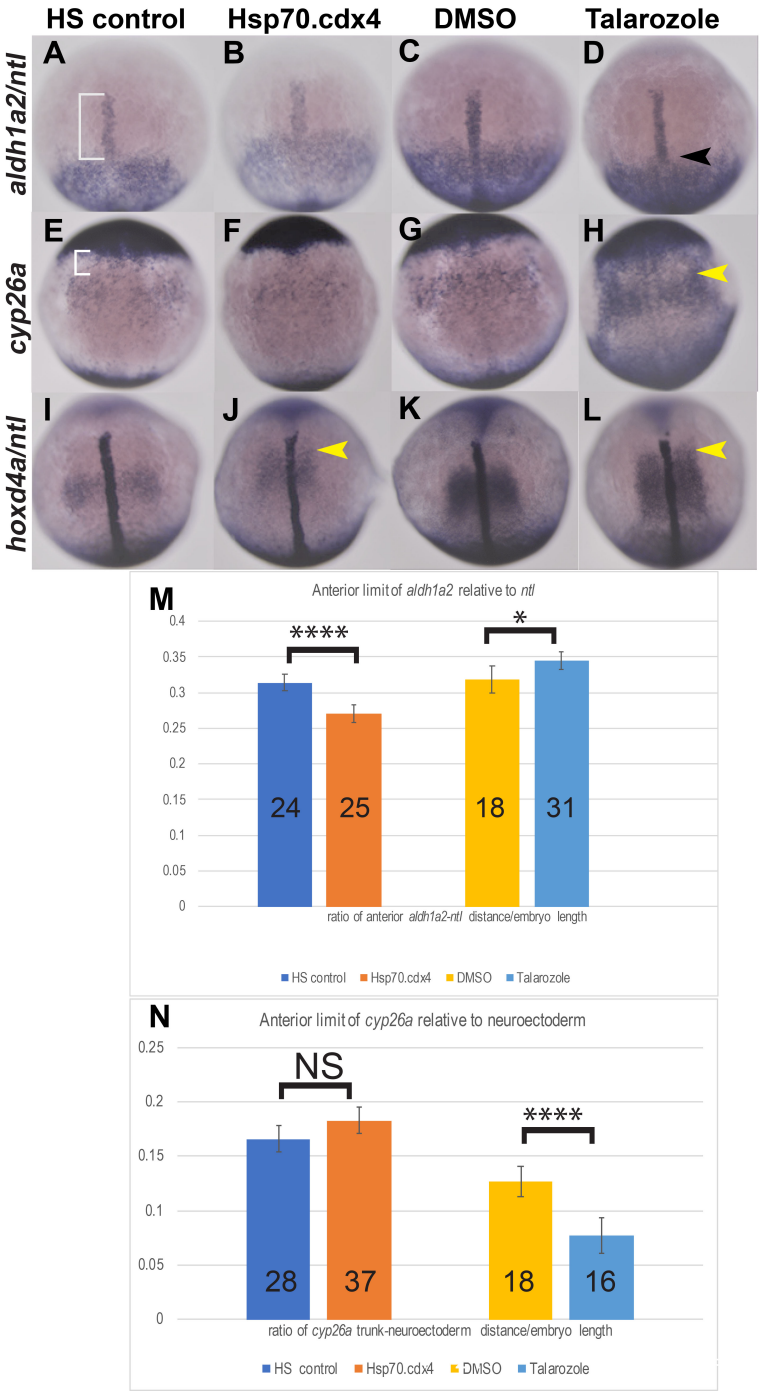

Fig.3.6. Transient increases in Cdx4 of RA have different effects on gene expression at the tailbud stage. In situ hybridization for *aldh1a2* (A-D) relative to the notochord shows the length between the anterior boundary of *aldh1a2* and *ntl* (white bracket, A) shifts rostrally in Hsp70.cdx4 (B) compared to HS controls (A). *Aldh1a2* expression shifts caudally in Talarozole-treated embryos (black arrowhead, D) compared to DMSO-treated controls (C). The *aldh1a2-ntl* gap was measured and normalized relative to the yolk diameter in M. (E-H) Expression of

Fig.3.6 (continued) *cyp26a* in trunk mesoderm relative to the anterior neuroectoderm is unaffected in Hsp70.cdx4 (F) compared to HS controls (white bracket, E). *Cyp26a* expression the trunk mesoderm of Talarozole-treated fish (H) is upregulated and shifted rostrally compared to DMSO-treated controls (G). The length between expression in the trunk mesoderm and neuroectoderm was quantified in N (measured area indicated by white bracket in E. (I-L) Expression of *hoxd4a* is shown relative to *ntl* and rostral shifts are indicated by yellow arrowheads (J,L). Statistical significance was calculated using student t-test (*, $p < .05$, ****, $p < .00001$). Non-significant differences are indicated NS.

3.3.7 Cdx-deficiency results in a caudal shift in aldh1a2 expression

Cdx deficiency results in a caudal expansion, rather than a shift of the whole fin field (Fig.3.4 J). In Fig.3.6, increased Cdx4 or RA resulted in different effects on *aldh1a2* and *cyp26a,* but a similar rostral shift in *hoxd4a*. I compared gene expression between wild type and Cdx-deficient embryos using same markers examined in Fig.3.6, namely *aldh1a2, ntl, cyp26a and hoxd4a*. As previously mentioned, a prior study fate-mapped the pectoral fins to a region adjacent to *aldh1a2* [33]. I therefore examined the *aldh1a2* boundary as in Fig.3.6. In wild type embryos, viewed dorsally, there was gap between the anterior limit of *aldh1a2* and *ntl* expression (Fig.3.7 A). This gap was increased in Cdx-deficient embryos, a result of the *aldh1a2* boundary shifting posteriorly (Fig.3.7 B). I quantified and compared theses length measurements and saw a small but significant increase in Cdx-deficient embryos relative to the anterior boundary of the notochord (Fig.3.7 G, p-value<.05). I also examined expression of *cyp26a* and *hoxd4a,* both of which are normally expressed directly anterior to *aldh1a2* [26], [56]. I compared the trunk expression of *cyp26a* relative to expression in the neural ectoderm and saw no change (Fig.3.7 C, D). I quantified the length between expression in the trunk and neuroectoderm, normalized to the diameter of the yolk and observed no significant difference (p-value>.05, Fig.3.7 H). While the anterior boundary of *cyp26a* was unaffected, the posterior boundary of trunk *cyp26a* expression was expanded caudally in Cdx-deficient embryos at this stage (Fig.3.7 D). This expansion of *cyp26a* has been well documented at later developmental stages in Cdx-deficient embryos [61], [62], [89]. I also examined *hoxd4a* expression at 1-2ss. Compared to wild type, the expression pattern of *hoxd4a* in Cdx-deficient embryos showed a caudal expansion of the posterior *hoxd4a* boundary, similar to that observed for *cyp26a* (black arrowhead in Fig.3.7 F). These results suggest that levels of high RA shift posteriorly in Cdx-deficient embryos and that this is accompanied by an expansion of the

posterior boundary of genes expressed more rostrally. These expanded genes reflect the later effects I observe in the pectoral fin field.

.

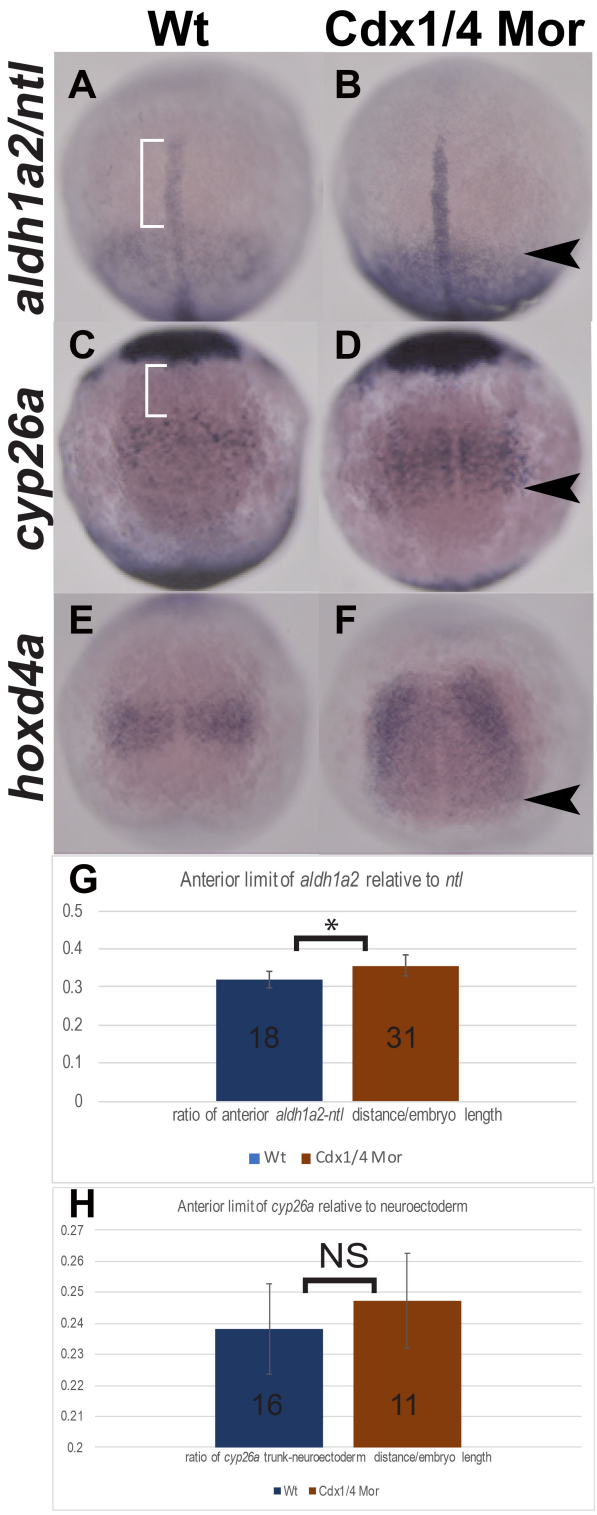

Fig.3.7 Cdx-deficiency results in a caudal shift in *aldh1a2* and caudal expansion of *cy26a* and *hoxd4a at* the tailbud stage (A-F). In situ hybridization for *aldh1a2* (A-B), *cyp26a* (C-D), at the

Fig.3.7 (continued) tb stage and *hoxd4a* at 1-2ss (E-F). Expression of *aldh1a2* relative to the notochord shows a caudal shift in Cdx-deficient embryos (black arrowhead, B), compared to wt (white brackets, A). The length between the anterior boundary of *aldh1a2* and the notochord was measure (white brackets) and normalized to the yolk diameter. No significant differences were observed (G). Expression of *cyp26a* in trunk mesoderm was compared relative to expression in anterior neuroectoderm (C,D). The rostral boundary of *cpy26a* in the trunk was unaffected in Cdx-deficient embryos (D) compared to wt (C), although the posterior boundary of *cyp26a* expanded caudally. The length between *cyp26a* in the trunk mesoderm and neuroectoderm (white bracket in C) was measured and normalized to the yolk diameter. Quantifications are shown in H and no significant differences were observed. Expression of *hoxd4a* is expanded caudally in Cdx-deficient embryos (black arrowhead, F), compared to wt (E). Statistical significance was calculated by using the student t-test, (*, $p < .05$). Non-significant differences are indicated NS.

3.4 Discussion

3.4.1 Gastrulation is a developmental window for studying limb placement along the A-P axis

RA and Cdx have been proposed to act directly through *Hox* genes in patterning tissues along the AP axis. In agreement with this, deletion of entire *Hox* paralogs results in transformations in segments of the axial skeleton [80], [174]. In addition, intriguing correlations between *Hox* expression and forelimb/hindlimb positioning across different species supports a model where a combination of *Hox* genes also establish position of the limbs [136], [175], [176], [177], [178]. With the exception of mutations in the *Hoxb5* gene, targeted deletion of entire paralogous groups of *Hox* genes in mice has no effect on the AP position or size of the forelimbs [145], [146]. Thus, it is still unclear what role specific Hox genes play in forelimb position As an alternative to studying just 1 HOX paralogous group, I focused on upstream regulators that control multiple paralogous groups. My goal was to identify a precise window when these regulators could alter limb position. In zebrafish, prolonged depletion or increase in RA levels leads to various pectoral fin phenotypes as well as severe effects on other developmental processes. To prevent unwanted secondary effects on development I limited the time in which RA levels accumulated in the embryo by treating them with Talarozole for brief 1hr intervals. I saw this was sufficient to alter the position of the pectoral fin from somite levels 2-3, to the region rostral to somite 1 (Fig.3.1 B,D). In contrast to a prior study where complete loss of Cyp26a led to underdeveloped pectoral fins, in our study, transient inhibition of Cyp26a with Talarozole does not affect the overall size of the pectoral fin [158]. There was an expansion of *shh* in the posterior fin mesenchyme of Talarozole-treated embryos (Fig.3.1 B) but loss of *shh* or expression or ectopic anterior expression was never observed. These severe effects were previously observed in embryos with teratogenic levels of RA [154].

My data suggest the position of the pectoral fins is primarily affected during gastrulation. One hour Talarozole treatments beginning at 4hpf are sufficient to shift the pectoral fins anteriorly (Fig.3.1 E). The frequency of these shifts reaches over 90% when Talarozole treatments were performed at 4hpf or 7hpf (gastrulation) while treatments at 11hpf (post gastrulation) led to a significant drop in the frequency of rostral fin shifts to 20%. Studies suggest gastrulation is also a critical window where RA is needed for the limb field to form in other organisms [114]. Early RA supplementation during embryonic day 8 (immediately after gastrulation) can also rescue the loss of *Tbx5* expression in the limb field of RA deficient mice [120]. In chick, inhibition of RA signaling between HH stage 4 and stage 8 is sufficient shift *tbx5a* expression in the LPM caudally by 2 somites [114], [120]. I also show that overexpression of Cdx4 alters pectoral fin position (Fig.3.2 C,D,G,H). This differs from a mouse study where increased levels of CDX1 led to reduced and underdeveloped forelimbs [78]. These transgenic mice overexpressed *Cdx1* continuously, so these phenotypes likely resulted in part from abnormalities that arose during outgrowth. The limb field was not examined in these embryos. In this study, I showed that overexpression of Cdx4 for 1 hour beginning at 7hpf led to a majority of larvae with rostral pectoral fin shifts (Fig.3.2 I). In these embryos, the gene expression patterns of *shh* and *tbx5a* were both unchanged relative to HS controls, which suggests that these fin buds were normal is size and polarity (Fig.3.2 C,D,G,H). The lack of patterning and outgrowth related phenotypes such as underdeveloped fins suggest overexpression at this developmental stage primarily effects positioning of the limb field and does not result in later developmental effects.

Overall, I developed a novel approach for studying limb position. Limiting potential downstream candidates of RA and CDX based on the developmental window I described will be informative in advancing the understanding of which additional factors contribute to limb positioning. There is also evidence for a late developmental window where limb positioning can be refined by the CUX1/2 pair of transcription factors in chick at HH stage 13 (post gastrulation) [179].

3.4.2 Tbx5a expression relative to numerous landmarks suggests the pectoral fin field is shifted along the AP axis

Previously, Mao and colleagues [113] used single cell labeling methods to identify the area of the lateral plate mesoderm (LPM) adjacent to somite levels 1-4 as giving rise to the mesenchymal portion of the later forming pectoral fin bud. Importantly, prior studies showed that the early expression of either *hand2* or *tbx5a* in the LPM at the level of somite 1-4 overlapped with the fate-mapped LPM cells that will become the fin bud [79], [86], [195], [204], [218]. Therefore, *tbx5a* is a reliable marker for the fin field in wild type zebrafish embryos. I characterized the expression of *tbx5a* relative to multiple embryonic landmarks as a useful read out for the effects of increased RA and Cdx4 on position of the fin field. I characterized the expression of *tbx5a* relative to the somites (Fig.3.3 M-P). In zebrafish, somite formation has been shown to progress normally in RA-deficient embryos, and in Cyp26a mutants, somite related defects were not reported, suggesting that the relative shifts I observe are not due to somite abnormalities [168]. In addition, whereas Cdx4 mutants do form smaller sized posterior somites, the anterior somites, which I use in assessing fin position, are not altered in size [82]. The fin field, which normally resides at the level of somites 1-4, shifts rostral to somite 1 in both

Talarozole treated and heat-shocked induced *Tg[phsp70:cdx4]* embryos at 18hpf (Fig.3.3 M-P).

RA has been implicated in eye morphogenesis but the AP position of the eye is unaffected in RALDH mutants [181], [182]. In zebrafish, high concentrations of exogenous RA treatment leads to duplications of the lens along the DV axis but no effects along the AP axis [183]. Therefore, I used the eye, also marked by *tbx5a* as a landmark in examining the anterior boundary of the LPM that expresses *tbx5a*. At 14hpf, the anterior LPM expression shifts anteriorly, closer to the eye in both Talarozole-treated and heat-shocked induced *Tg[phsp70:cdx4]* embryos (Fig.3.3 E-H).

I also used expression of *ntl* in the notochord as a landmark for comparing gene expression at the tailbud and 1-2ss stages. In Raldh2 mutants, the anterior boundary of the notochord appears just rostral to the level of rhombomeres 3 and 5, similar to wild type [42]. This suggests the anterior notochord is not affected by mis-regulation of RA and was a reliable landmark. In Cyp26a mutants and embryos treated with excess RA, reduced levels of *ntl* expression are seen in the posterior region of the embryo, which is a result of defects in growth of the tailbud. Meanwhile, expression of *ntl* in the anterior notochord is not affected [158], [184]. Post gastrulation, the RA and Cdx target gene *hoxd4a* is shifted rostrally, relative to the notochord in both Talarozole-treated and heat-shocked induced *Tg[phsp70:cdx4]* embryos (Fig.3.6 J,L). These expression patterns correlated with the rostral *tbx5a* shifts I later observe in the LPM at 14hpf (Fig.3.3 E-H,M-P). Although I cannot rule out the possibility of subtle effects to any of the landmarks used, the consistent shifts I observe relative to all three landmarks suggests that the AP position of the pectoral fin field is affected.

The effects on *tbx5a* that I describe relative to several landmarks are further corroborated by how the pattern of gene expression in the aLPM rostral to the fin field is affected.

Accompanying the rostral shift of *tbx5a* at 14hpf (Fig.3.3 E-H), I observe that the AP length of *scl-1* expression in the LPM rostral to *tbx5a* is significantly reduced in both heat-shocked induced *Tg[phsp70:cdx4]* and Talarozole-treated embryos (Fig.3.3 B, D). Cranial vascular precursors were previously fate mapped to this anterior *scl-1* region and Cyp26a/c double deficient embryos later form a reduced number of cranial vascular progenitors. This suggests that in Talarozole-treated and heat-shocked induced *Tg[phsp70:cdx4]* embryos, the entire LPM is not simply shifting anteriorly but subsets of LPM derivatives are being re-positioned, possibly at the expense of the *scl-1* expression in the LPM. Together, the landmarks used and the expression pattern of genes in the LPM suggest that increases in RA or Cdx4 are sufficient to shift the AP position of *tbx5a* expression in the early embryo that later result in rostral shifts of the pectoral fin buds.

3.*4.3. Cdx paralogs and RA act in parallel to restrict AP position of the fin field*

Prior studies related to development of various tissues have revealed distinct mechanisms through which RA and Cdx paralogs can act. In the neuroectoderm, RA and Cdx4 act antagonistically with one another to properly position the hindbrain-spinal cord transition. Meanwhile, in the intermediate mesoderm, Cdx paralogs act through the RA pathway to pattern the pro-nephrose into proximal and distal segments. In this study, Cdx paralogs are also necessary to promote high levels of RA in the anterior trunk mesoderm (Fig.3.7 A-B). However, key differences between Talarozole-treated and heat-shocked induced *Tg[phsp70:cdx4]* embryos suggest Cdx4 can also act on the pectoral fin field independently of the RA pathway (Fig.3.8). A rostral shift in *hand2* expression in the aLPM of Cyp26a+c deficient embryos was previously reported [169]. In this study, I saw a similar rostral shift of *hand2* expression in Talarozole-

treated embryos. Meanwhile, I did not see any effect on *hand2* expression in heat-shocked induced *Tg[phsp70:cdx4]* embryos (Fig.3.3 J), inconsistent with a mechanism where Cdx4 ultimately results in increased RA. Secondly, in Talarozole-treated embryos there is a clear rostral shift in *cyp26a* expression (Fig.3.6 H,N). Importantly, *cyp26a* is highly responsive to changes in RA. Yet, *cyp26a* was unaffected in heat-shocked induced *Tg[phsp70:cdx4]* embryos (Fig.3.6 N). This is not in conflict with the caudal expansion of *cyp26a* in Cdx-deficient embryos (Fig.3.7 D). In a prior study, interactions between Cdx4 and RA differed based on spatial context such that RA could repress *cdx4* expression rostral to the hindbrain-spinal cord transition but not caudal to it [61], [90]. Lastly, the temporal window in which I observe rostral pectoral fin shifts in heat-shocked induced *Tg[phsp70:cdx4]* embryos argues against a two-step process where Cdx4 only acts through the RA pathway to regulate the pectoral fin field. A late increase in RA, beginning at 11hpf results in a large decline in frequency of pectoral fin shifts to less than 20% (Fig.3.1 E). Meanwhile, at 11hpf, increased levels of Cdx4 leads to more than 2x the frequency of rostral pectoral fin shifts (40%). This suggests Cdx4 can influence the pectoral fin field past 11hpf when RA is no longer as effective. In a sequential pathway scenario where Cdx4 only acts through RA, I would have expected increased Cdx4 to be less effective than RA at 11hpf. Together, these observations argue for a pathway where Cdx4 can promotes RA and then in parallel, RA and Cdx4 can both restrict the limb field (Fig.3.8). This implies that an increase in either RA or Cdx4 is sufficient to alter the position of the pectoral fin field and that RA and Cdx4 could compensate for each other. Although RA is still present to restrict the pectoral fin field in Cdx-deficient embryos, the anterior *aldh1a2* boundary is shifted caudally, explaining why the posterior fin field boundary eventually expands caudally in the LPM of these embryos (Fig.3.4). An implication of this model is that in the absence of RA, the pectoral fin field

boundary would still be established. Prior studies showed the pectoral fin loss in RA deficient fish could be rescued by loss of Fgf signaling [53], [119], [127]. The position and size of the fin buds were not described in these embryos. One predication is that Cdx1a/Cdx4 still restrict the fin field from expanding further posteriorly.

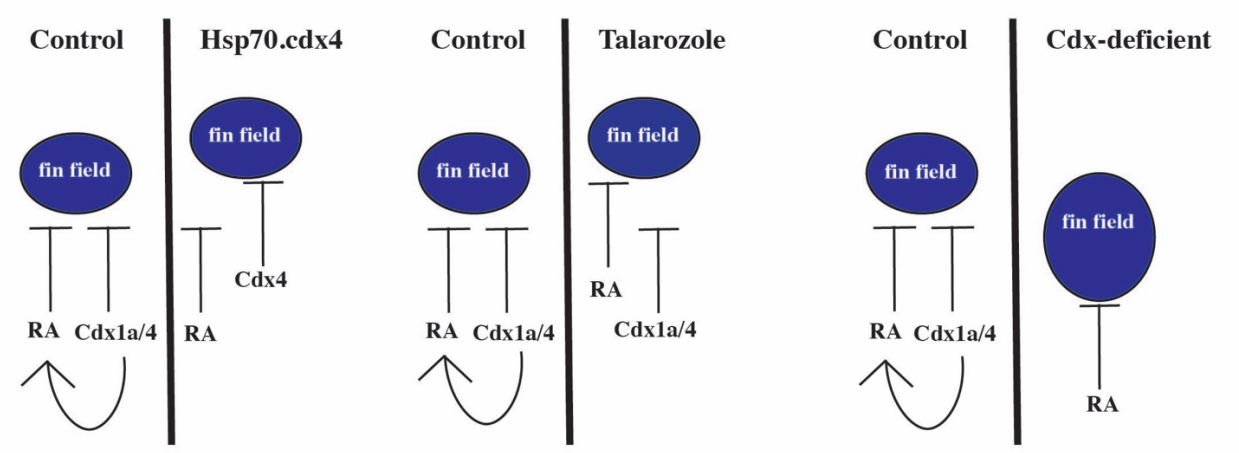

Fig.3.8 Cdx paralogs and RA act in parallel to restrict the pectoral fin field. (A) The posterior boundary of the fin field (inhibitory arrows in black) is determined by repressive effects of high RA or Cdx1a/Cdx4 levels in controls. Heat shock-induced Cdx4 over expression is sufficient to shift the fin field independently of RA. Talarozole treatment results in a rostral shift in high RA levels that is also sufficient to shift the fin field rostrally, while Cdx1a/4 levels are unchanged. (D) In controls, Cdx1a/Cdx4 promotes high levels of RA (black arrow) which then acts on the fin field in parallel with Cdx paralogs. In Cdx-deficient embryos, there is a caudal shift in RA, which allows the posterior boundary of the fin field to shift rostrally while the aLPM markers are unaffected.

3.4.4 Cdx-deficient embryos have patterning and migration defects in the pLPM

In zebrafish, Cdx-deficient embryos fail to properly pattern the endoderm, as well as the neural ectoderm [88], [175], [194]. In mice, loss of *Cdx* genes lead to ectopic expression of numerous cardiac associated genes, suggesting *Cdx* genes may play a role in the general patterning near the limb field region [99]. In Cdx-deficient zebrafish embryos, the anterior pectoral fin bud shifts caudally by a somite level, whereas the posterior boundary of the pectoral fin buds significantly expands caudally to the level of somite 6 (Fig.3.2 A-B,E-F). However, there was no effect on pectoral fin size when Cdx4 was overexpressed (Fig.3.2 C-D,G-H). To examine possible patterning defects related to pectoral fin development, I characterized the pattern of gene expression in the LPM of Cdx-deficient embryos prior to the migration of the fin field. The rostral boundary of *tbx5a* expression was not changed along the AP axis, relative to the eye or the somites (Fig.3.4 D-F,K-L). Similarly, the expression length of *scl-1* rostral to *tbx5a* was unaffected (Fig.3.4 A-C). This was surprising, given the caudal shift in the fin bud I later observed in Cdx-deficient embryos. At 18hpf, the posterior boundary of *tbx5a* expression is visibly expanded caudally along the LPM from the level of somite 4 in wild type to the level of somites 7-8 in Cdx-deficient embryos (Fig.3.4 I, J). Meanwhile, the *hand2* gene which is normally expressed in the pLPM partially overlapping with *tbx5a* is also expressed throughout the LPM posterior to the fin field (Fig.3.4 G). In Cdx-deficient embryos, the expression length of *hand2* along the AP axis is significantly reduced in the pLPM (Fig.3.4 H). Previous fate-mapping of the pLPM immediately posterior to the fin field at somite level 5 suggests this region contains LPM cells that contribute to the peritoneum [113]. Identification of reliable genetic markers for the peritoneum and more extensive fate-mapping of this LPM region at this stage will allow for better characterization of the patterning defects associated with Cdx-deficiency.

CHAPTER 4

DISCUSSION

4.1 Conclusions

The primary conclusion from my work is that the zebrafish pectoral fin field is established during gastrulation. This conclusion is supported by the experimental manipulation of two separate developmental pathways. Increasing levels of RA or Cdx4 both provided the same answer; the position of the fin field could be shifted rostrally prior to the end of gastrulation. The similar effects of increased RA and Cdx4 suggest they each restrict the fin field from forming further caudally. Meanwhile, the pectoral fin field expanded caudally in Cdx-deficient embryos, which further corroborates the restrictive role of Cdx in formation of the fin field.

A second conclusion from this work is that Cdx factors act in parallel with RA in regulation of the fin field. Prior studies showed that increased RA does not affect the expression of *cdx4*. Two key observations from my work suggest that Cdx4 does not act upstream of RA. The first is that the effects of transiently increasing levels of Cdx4 or RA at 4,7 and 11hpf showed that Cdx4 acts on pectoral fin position at a slightly later time compared to RA (compare Fig.3.1 E and Fig.3.2 I). Specifically, increasing RA levels beginning at 4hpf and 7hpf led to a high frequency of rostral fin shifts that was not observed when RA levels were increased at 11hpf. In contrast, increased levels of Cdx4 did not result in a high frequency of rostral fin shifts until 7hpf and there was still a moderate frequency of rostral fin shifts when Cdx4 levels were increased at 11hpf. Overall, this suggests RA and Cdx4 act in slightly staggered windows and that RA acts earlier than Cdx4.

The second observation was that Talarozole mediated increase in RA leads to rostral

shifts in RA responsive genes such as *cyp26a* at the tailbud stage and *hand2* at 14hpf, both of these genes where unaffected by increased levels of Cdx4. This suggests that overexpression of Cdx4 does not result in an increase in RA levels. One conflicting finding was that increased Cdx4 did result in a rostral shift of *aldh1a2* expression which suggests levels of RA do shift rostrally, but this was not sufficient to promote a rostral shift in RA responsive genes. Because my study was limited to assessing changes to RA indirectly from gene expression patterns, a reliable method for direct visualization of RA during early zebrafish development would have helped in definitively concluding that Cdx4 does not act through an increase in RA to influence position of the fin field.

From this study, I could not definitively conclude whether a subset of the pectoral fin field, marked by *tbx5a*, is compromised in migration to the fin bud in Cdx-deficient embryos. In wild type, *tbx5a* expressing cells reliably form at the level of somites 1-4 and these cells all migrate into the fin bud. In Cdx-deficient embryos, *tbx5a* expressing cells are expanded to the level of somites 1-8. However, cells at the level of somites 7 and 8 fail to reliably migrate from the LPM into the pectoral fin bud. There are two possible explanations for why cells at somite levels 1, 7 and 8 don't reliably contribute to the fin bud. The first is that *tbx5a* is not specifically marking the fin field anymore. The second is that cells at somite levels 7 and 8 were too far to respond to signals that direct migration of the fin field. The fin field is normally directed to the fin bud region by *fgf24*, which is expressed at somite levels 2-3 in wild type and at somite levels 2-6 in Cdx-deficient embryos (Fig.3.3 E-F). The *tbx5a* expressing cells at somite levels 7 and 8 were 3-4 somite lengths from where *fgf24* was expressed at 18hpf (somite levels 2-4). In wt, the fin field cells that migrate towards fgf24 are only 1-2 somite lengths away. Based on the reliable expression of *tbx5* in the limb progenitors across various species, the latter explanation seems

much more likely. To confirm this, Fgf-soaked bead implantations can be used. The hypothesis is that cells at somites 1,7 and 8 would migrate towards an implanted Fgf-soaked bead in proximity.

4.2 Future Directions

4.2.1 Characterizing the role of RA and cdx genes in specification of motor neurons and muscle progenitors associated with the pectoral fin

The bone, muscle, and neural tissues associated with the pectoral fin must coordinate their development to result in a functional fin that allows for locomotion of the adult. Motor neurons associated with the pectoral fin are specified in a region of the spinal cord called the lateral motor column (LMC) [185]. In chick as well as mouse, cross-regulatory interaction between *HOX* genes are necessary for LMC identity such that *HOX6* genes promote LMC identity while *HOX9* repress LMC identity, in part through repression of *HOXC6* [186], [187], [188]. Meanwhile, changes in limb position have no clear effect on where LMCs form in the spinal cord [144]. In zebrafish, increased levels of RA and Cdx4 are both sufficient to shift *hox* expression to more rostral locations in the spinal cord, which suggests that increased levels of RA or Cdx4 would result in a rostral shift in the position of the LMC through *hox6/hox9* or other *hox* genes. To test this in zebrafish, I would perform retrograde labeling by injecting dye into the fin which would subsequently diffuse along the axons to the cell body [189]. I would expect that retrograde labeling in embryos with increased levels of RA or Cdx4 to result in labeling of motor neurons located more anteriorly in the spinal cord. Meanwhile, *hox* genes are expressed more posteriorly in Cdx-deficient embryos. Retrograde labeling of axons in Cdx-deficient embryos would result in labeling of motor neurons located more posteriorly in the spinal cord.

The muscles that populate the forelimb initially form at a specific location in the somites and later migrate into the limb. However, transplanting LPM from the limb region to a region where the limb normally does not form can induce an ectopic limb. Interestingly, these LPM transplants can also re-specify the surrounding somites to later form limb muscle [190]. This suggests that a rostral shift of the fin field in zebrafish may be sufficient to re-specify the nearby somites to form muscles of the fin. To test this, I would live image embryos with transgenic lines that label the somites and identify the somite region that pectoral fin muscles originate from in embryos with increased RA or Cdx4. The muscle progenitors of the pectoral fin are normally specified in somites 3 and 4, which corresponds to the level where the posterior half of the fin field is located [191]. In embryos with increased RA or Cdx4, the fin field forms rostral to somite level 1, meaning that somite 1 is the closest to where the posterior fin field is located. This suggests that somite 1 is likely where muscle progenitors of the fin originate from. In Cdx-deficient embryos, it is unclear whether the posterior fin field extends to somite level 6 or somite level 8. If pectoral fin muscles originate at the level of the posterior half of the fin field, I would expect muscle progenitors to originate from somites 3-6 or somites 4-8 in Cdx-deficient embryos.

4.2.2 Examine whether Cdx and Fgfs regulate pelvic fin position

In tetrapods, the hindlimbs are always positioned along the body axis at the level of the anal region. In fish, the pelvic fins are the homolog to the hindlimb but in contrast to hindlimbs, pelvic fin position can vary across species from abdominal, thoracic to jugular regions [192]. There is also a significant delay in formation of the pelvic fins. While the pectoral fins form in the first few days of zebrafish development, the pelvic fins aren't visible until after 3 weeks

[193]. Thyroid hormone signaling initiates the transition from larval to juvenile stage at this time and has also been proposed to be critical for initiating pelvic fin formation [194]. In tetrapods, *Hox9* genes are expressed in the LPM at the level where the hindlimb forms and in fish, there is a second wave of *hox9* expression in LPM when larvae undergo metamorphosis to the juvenile stage, just before the pelvic fins form [195]. This is an important observation because Cdx4 is required for the normal expression of *hox9* genes during embryonic stages [83]. If Cdx4 can also mediate changes in *hox9* expression at 3 weeks, increased levels of Cdx4 may result in rostral shifts of the pelvic fins. To test this, I would transiently increase Cdx4 levels prior to, during and after three weeks post fertilization. I would then examine where the pelvic fins form in these fish. I would expect to see a rostral shift in the expression region of *hox9* genes and a rostral shift in the pelvic fin pelvic fins.

In zebrafish and nile tilapia, the LPM region that later contributes to pelvic fins undergoes a dramatic displacement from the initial location in the embryo at somite level 14 to somite level 8, where the pelvic fins eventually form [196]. The determinants of this long-range displacement are unknown. Fgf24 can only mediate short-range movement of the pectoral fin progenitors from the LPM to the fin bud in zebrafish, but other Fgfs are known to regulate long-range migration, as seen in migration of neuromast progenitors [197]. To test whether any Fgf signaling is necessary for displacement of the pelvic fin progenitors from somite level 14 to somite level 8, I would use a transgenic line to drive activation of a dominant negative Fgfr [198]. One possible outcome is that loss of Fgf signaling leads to reduced displacement of the pelvic fin field cells and later results in pelvic fins that are either delayed or reduced in size. These results would have interesting implications for the loss of pelvic fins in pufferfish [199]. A large displacement of LPM cells is observed in these fish but there is currently no explanation for

why pelvic fins ultimately fail to form, although the long-range displacement is believed to be related [199]. If Fgf signaling is important for the displacement of the pelvic fins in zebrafish, it would suggest that changes or loss of Fgf signaling may also underlie loss of the pelvic fins in puffer fish.

4.2.3 Examine whether the Bmp pathway acts upstream of RA to regulate the fin field

Transient loss of Bmp signaling via inducible *noggin* expression or a pharmacological inhibitor of Bmp signaling (LDN-193189) are each sufficient to induce ectopic pectoral fins in zebrafish that appear smaller in size [200]. The mechanism by which Bmp inhibition promotes these extra pectoral fins is unknown. However, transient application of exogenous RA can also result in pectoral fin duplications in zebrafish embryos [102]. Importantly, a separate study showed that a high concentration of Bmp inhibitor drug is sufficient to change the pattern of *cyp26a* and *aldh1a2* expresion during late gastrulation [33]. These findings suggest that Bmp may regulate pectoral fin development through effects on *aldh1a2* and *cyp26a* expression. To test this, I would perform refined Bmp inhibition experiments that are limited to 1 hr as I did for Talarozole treatments in this thesis. I would begin prior to 4hpf, where I already showed that increased RA leads to a high frequency of rostral fin shifts.

The proposed study discussed above would address whether Bmp acts upstream of RA. One important assumption is that the fin field is in fact duplicated by18hpf and that specification of the fin field is compromised. An unexpected, but possible alternative is that mis-regulation of Bmp signaling does not affect specification of the fin field at all. This would implicate effects on migration of the fin field as the reason for the additional fins. To test this, I would characterize expression of *fgf24* and live image embryos treated with the Bmp inhibitor. Importantly, the

duration of Bmp inhibitor treatments that result in fin duplications began during gastrulation and extended into somitogenesis stages. This means that *fgf24* expression that begins at 18hpf may in fact be affected.

Although *fgf24* is present in fish, this specific *Fgf* is not present in the mouse genome [201]. This is intriguing because mis-regulation of Bmp signaling is not associated with ectopic limbs in mouse. Other branches of the Tgf-beta pathway result in a related duplication of the forelimb in mouse although it is not understood how these phenotypes arrise either [202], [203], [204], [205], [206].

4.2.4 Test whether hox genes act downstream of Cdx4 to repress formation of the fin field

Ectopic expression of *hox8* rescues hematopoietic defects in Cdx-deficient zebrafish embryos [82]. In mice, *Hox8* genes can also rescue the posterior elongation defect in Cdx-deficient embryos [87]. The implication of these findings is that *hox* genes may also rescue the expanded fin field in Cdx-deficient embryos. Expression of *hoxc4, hoxc6* and hox*c8* genes is delayed in Cdx4 mutants at 75% epiboly [83]. One possibility is that these genes act downstream of Cdx4 to repress formation of the fin field. To test this, I would use existing heat shock inducible lines to overexpress these *hox genes* at 75% epiboly. Importantly, increased levels of Cdx4 affects the fin field at 60% epiboly (7hpf), just prior to when a number of these *hox* genes normally turn on.

4.3 Concluding remarks

A number of congenital limb defects (CLDs) in humans are still poorly understood. Many of these may result from abnormalities that arise before a limb bud is visible. There is still a huge

gap in our understanding of how the pre-limb bud stage is regulated and studies focused on this developmental time may help our understanding of how other CLDs arise. Studies of pectoral fin development in the early zebrafish embryo have already shown promise in helping us understanding why Holt-Oram syndrome patients commonly develop defects in the upper arm region. The rostral fin shifts I studied in this dissertation closely resemble limb defects in patients with Sprengel's deformity, a rare CLD that is characterized by a rostral shift of the shoulder blade and limb by 5-10cm. The cause of Sprengel's deformity is not well understood but patients often have vertebral abnormalities as well. My work on RA and Cdx in zebrafish might have implications for when defects associated with Sprengel's deformity first arise. Studies in the early zebrafish embryo may be useful for better understanding the cause of many other CLDs that have remained unresolved.

APPENDIX

A.1. Vascular progenitors are located at the site of splitting between the fin field and aLPM

The pectoral fin receives blood from the common cardinal vein, but little is known about how fin and vascular progenitors interact in order to integrate the two tissues into a functional organ. To examine possible interactions during the window where the pectoral fin field migrates into the fin, I live imaged *Tg(kdrl:mCherry), Et(hand2:eGFP)ch2* double transgenic embryos to simultaneously visualize the vascular progenitors (mCherry) and LPM (eGFP). At 20hpf, a small number of vascular progenitors are visible near the site where splitting of the fin field and aLPM occurs (Fig. A1. A). Splitting of the fin field from the adjacent aLPM is complete at 22hpf (Fig.A.1 B white asterisk). By this stage, vascular progenitors have populated the space between the fin field and aLPM (Fig. A.1 B white asterisk). Whether the vascular progenitors actively contribute to splitting of the fin and aLPM is unknown. One possibility is that vascular progenitors facilitate splitting of the LPM by adhering to the aLPM as well as the fin field and pulling the two regions apart. Alternatively, a repulsive signal from the vascular progenitors may promote clearance of LPM cells from the region between the fin field and aLPM. The proximity of the two cell populations and the physical contacts between the LPM and vascular progenitor at 22hpf supports these possibilities. Lastly, the fin field may influence the vascular progenitors by releasing a signal specifically at the splitting site in order to recruit vascular progenitors. This recruitment may be necessary to properly localize the common cardinal vein that later provides blood flow to the pectoral fin.

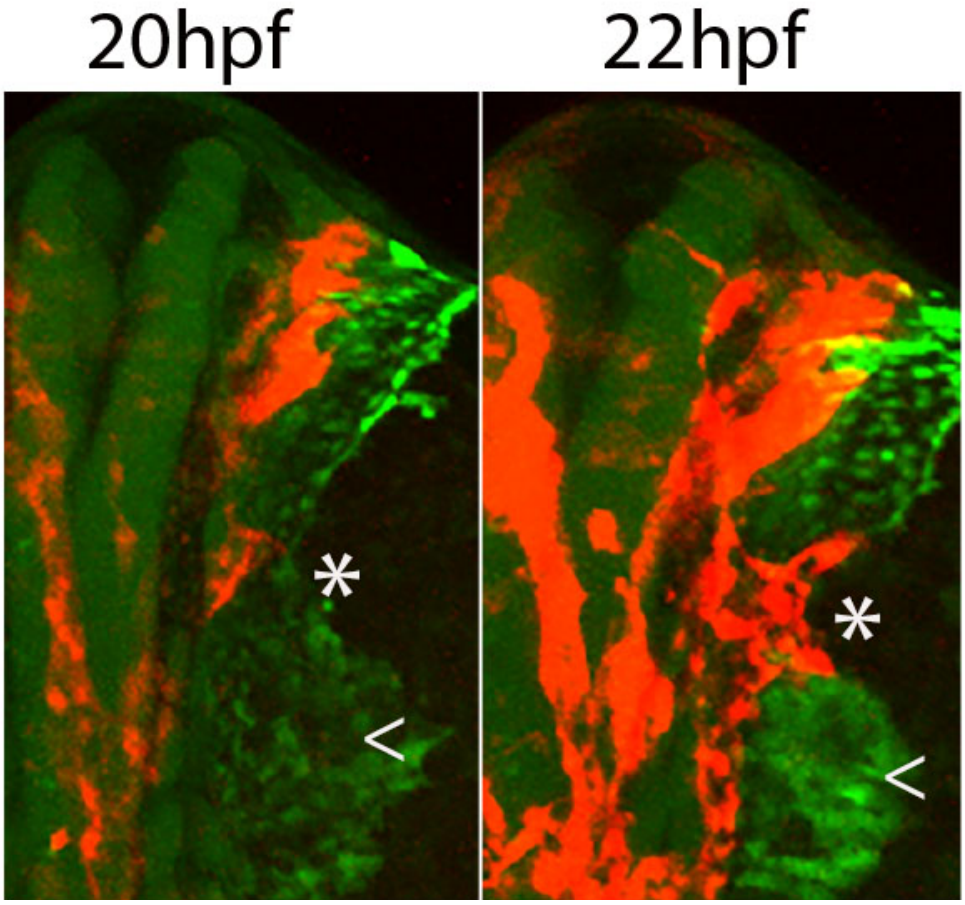

Fig.A.1 Vascular progenitors are located at the site of splitting between the fin field and aLPM. (A) Maximum intensity projections of *Tg(kdrl:mCherry), Et(hand2:eGFP)ch2* double transgenic embryos mark vascular (mCherry) and LPM cells (eGFP) at the junction (white asterisk) between the fin field (white arrowhead) and adjacent LPM (green) during mid-migration of the fin field at 20hpf-22hpf (dorsal view of right side). just prior to the splitting of the field and aLPM, a population of vascular progenitors (red) populate the junction between the aLPM and fin field (asterisk). (B) The fin field and aLPM have split by 22hpf (white asterisk) and vascular progenitors have migrated laterally to form two leading edges that make contact with the aLPM and the fin field (white arrowhead)

A.2 Increased levels of Cdx4 result in abnormal arrangement of differentiating cardiac cells

The characterization of gene expression in the aLPM in Fig.3.3, showed rostral shifts in heart related expression of *hand2* and *tbx5a* after RA levels are increased. In contrast, only *tbx5a* shifts rostrally after Cdx4 levels are transiently increased. This suggests that an increase in RA or Cdx4 has a different effect on cardiac lineages. This may result from direct effects on cell fates in the LPM or secondary effects that result from abnormal development of the endoderm, which influences cardiac migration [207], [208], [209], [210]. I examined the overall arrangement of differentiating cardiac cells at 20hpf using an antibody for myosin heavy chain (MHC). In HS controls, differentiating cardiac cells arrange normally at the midline (brown stain in Fig.A.2). In contrast, heat-shocked induced *Tg[phsp70:cdx4]* embryos showed an incomplete arrangement of the heart cone, where cells failed to fully arrange at the midline (Fig.A.2 B). This heart cone defect was observed in 24/80 embryos (Fig.A.2 H). A more severe delay in migration was seen in 12/80 embryos, while 11/80 had no MHC stain in the precursors. I saw a normal pattern of differentiating cardiac cells in DMSO-treated and Talarozole-treated embryos. However, Talarozole-treated embryos showed a mild disorganization at the center of the heart cone from where differentiating cardiac cells are normally excluded from. This suggests a mild defect in arrangement of these cells may also occur in Talarozole-treated embryos (Fig.A.2 C-D). Compared to wild type, Cdx-deficient embryos did not have an abnormal arrangement of differentiating cardiac cells although the AP position of the heart cone was not examined.

.

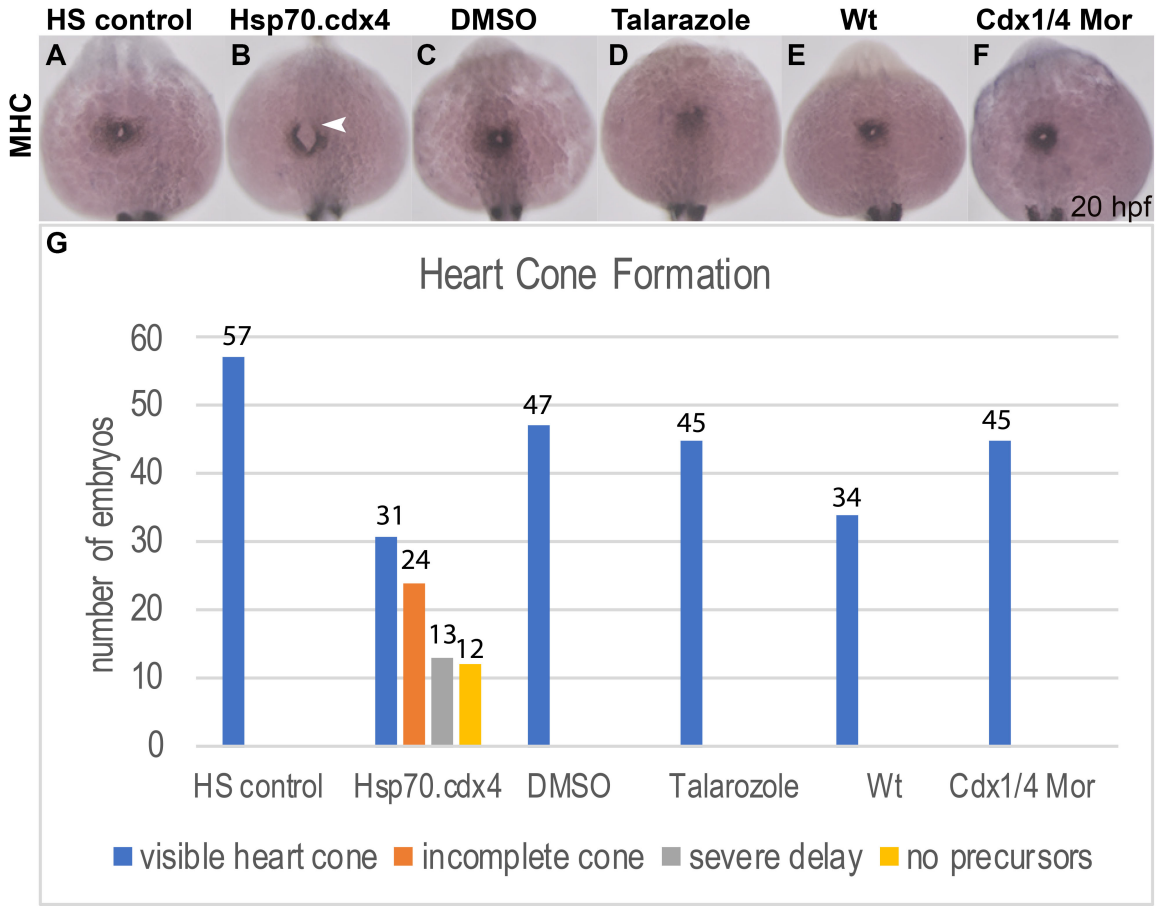

Fig.A.2 Increased levels of Cdx4 result in abnormal arrangement of differentiating cardiac cells. (A-F) Differentiating cardiac cells form a visible heart cone at the midline at 20hpf in HS controls (A), Hsp70.cdx4 (B), DMSO-treated (C), Talarozole-treated (E) , Wt (E) and Cdx-deficient (F). Hsp70.cdx4 fish form an incomplete arrangement of differentiating cardiac cells (white arrowhead, B). Quantification of the heart cone phenotypes show a range of severity for Hsp70.cdx4 (G). Number of embryos used is indicated above bars. Differentiating cardiac cells are marked with Myosin Heavy Chain (brown)

A.3. RA does not act upstream of cdx4 expression at 75% epiboly

Application of exogenous RA during segmentation stages was previously shown to have no effect on the normal expression of *cdx4*. At 75% epiboly expression of *cdx4* is normally strong on the ventral side of the marginal zone. To confirm that transient increases in RA don't affect *cdx4* expression along the ventral/dorsal margin, I compared *cdx4* expression between wild type and Talarozole-treated embryos. At this stage, embryos viewed laterally express *cdx4* at mildly higher levels at the ventral margin (asterisk, Fig.A.3 A). The pattern of expression at the ventral margin is not affected in Talarozole-treated embryos (Fig.A.3 B). As a positive control, heat shocked-induced Cdx4 embryos are shown, which express *cdx4* throughout the animal pole region (Fig.A.3 C). Expression of *cdx4* was also shown in prior studies to be normal in Cdx-deficient fish, which I confirm in Fig.A.3 D, where expression is unaffected [82].

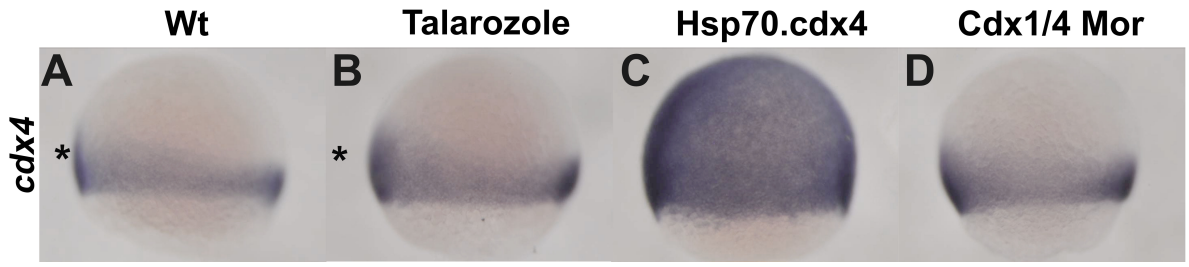

Fig.A.3. Increased RA does not act upstream of *cdx4* expression at 75% epiboly. In situ hybridization for *cdx4* at 75% epiboly shows that the mild increase in expression at the ventral margin in Wt (asterisk, A) is comparable to expression in Talarozole-treated (white arrowhead, B) or Cdx-deficient embryos (D). The expression of *cdx4* in Hsp70.cdx4 fish is seen throughout the animal pole and excluded from the yolk region. Embryos are oriented laterally, ventral to the left and animal pole towards the top.

REFERENCES

[1] R. G. Harrison, “Experiments on the development of the forelimb of amblystoma, a self differentiating equipotential system,” *J. Exp. Zool.*, vol. 25, no. 2, 1918.

[2] T. Yano and K. Tamura, “The making of differences between fins and limbs,” *J. Anat.*, vol. 222, no. 1, pp. 100–113, 2013.

[3] N. Shubin, C. Tabin, and S. Carroll, “Deep homology and the origins of evolutionary novelty,” *Nature*, vol. 457, no. 7231, pp. 818–823, 2009.

[4] C. Tickle, “How the embryo makes a limb: Determination, polarity and identity,” *J. Anat.*, vol. 227, no. 4, pp. 418–430, 2015.

[5] N. Mercader, “Early steps of paired fin development in zebrafish compared with tetrapod limb development,” *Dev. Growth Differ.*, vol. 49, no. 6, pp. 421–437, 2007.

[6] R. Zeller, J. López-Ríos, and A. Zuniga, “Vertebrate limb bud development: Moving towards integrative analysis of organogenesis,” *Nat. Rev. Genet.*, vol. 10, no. 12, pp. 845–858, 2009.

[7] F. Marlétaz, L. Z. Holland, V. Laudet, and M. Schubert, “Retinoic acid signaling and the evolution of chordates,” *Int. J. Biol. Sci.*, vol. 2, no. 2, pp. 38–47, 2006.

[8] V. Giguere, E. S. Ong, P. Segui, and R. M. Evans, “Identification of a receptor for the morphogen retinoic acid,” *Nature*, vol. 330, no. 6149, pp. 624–629, 1987.

[9] M. Petkovich, N. J. Brand, A. Krust, and P. Chambon, “A human retinoic acid receptor which belongs to the family of nuclear receptors,” *Nature*, vol. 330, no. 6147, pp. 444–450, 1987.

[10] T. Koide, M. Downes, R. A. S. Chandraratna, B. Blumberg, and K. Umesono, “Active repression of RAR signaling is required for head formation,” *Genes Dev.*, vol. 15, no. 16, pp. 2111–2121, 2001.

[11] R. Kurokawa *et al.*, “Polarity-specific activities of retinoic acid receptors determined by a co-repressor,” *Nature*, vol. 377, no. 6548, pp. 451–454, 1995.

[12] J. D. Chen and R. M. Evans, “A transcriptional co-repressor that interacts with nuclear hormone receptors,” *Nature*, vol. 377, no. 6548, pp. 454–457, 1995.

[13] V. Kashyap and L. J. Gudas, “Epigenetic regulatory mechanisms distinguish retinoic acid-mediated transcriptional responses in stem cells and fibroblasts,” *J. Biol. Chem.*, vol. 285, no. 19, pp. 14534–14548, 2010.

[14] T. E. Spencer *et al.*, “Steroid receptor coactivator-1 is a histone acetyltransferase,” *Nature*, vol. 389, no. 6647, pp. 194–198, 1997.

[15] J. A. Williams *et al.*, “Retinoic acid receptors are required for skeletal growth, matrix homeostasis and growth plate function in postnatal mouse,” *Dev. Biol.*, vol. 328, no. 2, pp. 315–327, 2009.

[16] S. Kumar and G. Duester, “Retinoic acid controls body axis extension by directly repressing Fgf8 transcription,” *Dev.*, vol. 141, no. 15, pp. 2972–2977, 2014.

[17] R. Studer, M., Pöpperl, H., Marshall, H., Kuroiwa, A. & Krumlauf, “Role of a Conserved Retinoic Acid Response Element in Rhombomere Restriction of Hoxb-1,” *Science (80-.).*, vol. 265, no. September, pp. 6–8, 1994.

[18] G. Duester, “Retinoic Acid Synthesis and Signaling during Early Organogenesis,” *Cell*, vol. 134, no. 6, pp. 921–931, 2008.

[19] L. M. Y. Lee *et al.*, “A paradoxical teratogenic mechanism for retinoic acid,” *Proc. Natl. Acad. Sci. U. S. A.*, vol. 109, no. 34, pp. 13668–13673, 2012.

[20] E. D’Aniello, P. Ravisankar, and J. S. Waxman, “Rdh10a provides a conserved critical step in the synthesis of retinoic acid during zebrafish embryogenesis,” *PLoS One*, vol. 10, no. 9, pp. 1–21, 2015.

[21] L. Feng, R. E. Hernandez, J. S. Waxman, D. Yelon, and C. B. Moens, “Dhrs3a regulates retinoic acid biosynthesis through a feedback inhibition mechanism,” *Dev. Biol.*, vol. 338, no. 1, pp. 1–14, 2010.

[22] G. Lupo *et al.*, “Retinoic acid receptor signaling regulates choroid fissure closure through independent mechanisms in the ventral optic cup and periocular mesenchyme,” *Proc. Natl. Acad. Sci. U. S. A.*, vol. 108, no. 21, pp. 8698–8703, 2011.

[23] O. Loudig, C. Babichuk, J. White, S. Abu-Abed, C. Mueller, and M. Petkovich, “Cytochrome P450RAI(CYP26) promoter: A distinct composite retinoic acid response element underlies the complex regulation of retinoic acid metabolism,” *Mol. Endocrinol.*, vol. 14, no. 9, pp. 1483–1497, 2000.

[24] O. Loudig, G. A. MacLean, N. L. Dore, L. Luu, and M. Petkovich, “Transcriptional co-operativity between distant retinoic acid response elements in regulation of Cyp26A1 inducibility,” *Biochem. J.*, vol. 392, no. 1, pp. 241–248, 2005.

[25] S. Reijntjes, A. Blentic, E. Gale, and M. Maden, “The control of morphogen signalling: Regulation of the synthesis and catabolism of retinoic acid in the developing embryo,” *Dev. Biol.*, vol. 285, no. 1, pp. 224–237, 2005.

[26] B. Dobbs-McAuliffe, Q. Zhao, and E. Linney, “Feedback mechanisms regulate retinoic acid production and degradation in the zebrafish embryo,” *Mech. Dev.*, vol. 121, no. 4, pp. 339–350, 2004.

[27] H. Fujii *et al.*, “Metabolic inactivation of retinoic acid by a novel P450 differentially expressed in developing mouse embryos,” *EMBO J.*, vol. 16, no. 14, pp. 4163–4173, 1997.

[28] R. J. White, Q. Nie, A. D. Lander, and T. F. Schilling, “Complex regulation of cyp26a1 creates a robust retinoic acid gradient in the zebrafish embryo,” *PLoS Biol.*, vol. 5, no. 11, pp. 2522–2533, 2007.

[29] T. Kudoh, S. W. Wilson, and I. B. Dawid, “Distinct roles for Fgf, Wnt and retinoic acid in posteriorizing the neural ectoderm.,” *Development*, vol. 129, no. 18, pp. 4335–46, Sep. 2002.

[30] F. CRICK, “Diffusion in embryogenesis,” *Nature*, vol. 225, no. 5233, p. 671, 1970.

[31] S. Shimozono, T. Iimura, T. Kitaguchi, S. I. Higashijima, and A. Miyawaki, “Visualization of an endogenous retinoic acid gradient across embryonic development,” *Nature*, vol. 496, no. 7445, pp. 363–366, 2013.

[32] K. Laue, M. Jänicke, N. Plaster, C. Sonntag, and M. Hammerschmidt, “Restriction of retinoic acid activity by Cyp26b1 is required for proper timing and patterning of osteogenesis during zebrafish development,” *Development*, vol. 135, no. 22, pp. 3775–3787, 2008.

[33] R. W. Naylor, L. B. Skvarca, C. Thisse, B. Thisse, N. A. Hukriede, and A. J. Davidson, “BMP and retinoic acid regulate anterior-posterior patterning of the non-axial mesoderm across the dorsal-ventral axis,” *Nat. Commun.*, vol. 7, pp. 1–14, 2016.

[34] J. G. Wilson, C. B. Roth, and J. Warkany, “An analysis of the syndrome of malformations induced by maternal vitamin a deficiency. Effects of restoration of vitamin a at various times during gestation,” *Am. J. Anat.*, vol. 92, no. 2, pp. 189–217, 1953.

[35] S. BURT WOLBACH., ANDPERCY R. HOWE, “TISSUE CHANGES FOLLOWING DEPRIVATION OF FATSOLUBLE A VITAMIN.,” vol. 22657, no. 1883, p. 22657, 1925.

[36] G. A. Thompson, J. N., Howell, J. M. & Pitt, “Vitamin A and reproduction in rats,” *J. Reprod. Fertil.*, vol. 8, pp. 270–271, 1964.

[37] D. Lohnes, P. Kastner, A. Dierich, M. Mark, M. LeMeur, and P. Chambon, “Function of retinoic acid receptor γ in the mouse,” *Cell*, vol. 73, no. 4, pp. 643–658, 1993.

[38] T. Lufkin *et al.*, “High postnatal lethality and testis degeneration in retinoic acid receptor α mutant mice,” *Proc. Natl. Acad. Sci. U. S. A.*, vol. 90, no. 15, pp. 7225–7229, 1993.

[39] D. Lohnes *et al.*, “Function of the retinoic acid receptors (RARs) during development. (I) Craniofacial and skeletal abnormalities in RAR double mutants,” *Development*, vol. 120, no. 10, pp. 2723–2748, 1994.

[40] P. and C. Niederreither, K., Subbarayan, V., Dollé, “Embryonic retinoic acid synthesis is essential for early mouse post-implantation development Karen,” *Nature*, vol. 128, no. 7, pp. 1019–1031, 1999.

[41] G. Begemann, T. F. Schilling, G. J. Rauch, R. Geisler, and P. W. Ingham, “The zebrafish neckless mutation reveals a requirement for raldh2 in mesodermal signals that pattern the hindbrain.,” *Development*, vol. 128, no. 16, pp. 3081–94, Aug. 2001.

[42] H. Grandel *et al.*, “Retinoic acid signalling in the zebrafish embryo is necessary during pre-segmentation stages to pattern the anterior-posterior axis of the CNS and to induce a pectoral fin bud.,” *Development*, vol. 129, no. 12, pp. 2851–65, Jun. 2002.

[43] R. E. Hernandez, A. P. Putzke, J. P. Myers, L. Margaretha, and C. B. Moens, “Cyp26 enzymes generate the retinoic acid response pattern necessary for hindbrain development,” *Development*, vol. 134, no. 1, pp. 177–187, 2006.

[44] M. Uehara *et al.*, “CYP26A1 and CYP26C1 cooperatively regulate anterior-posterior patterning of the developing brain and the production of migratory cranial neural crest cells in the mouse,” *Dev. Biol.*, vol. 302, no. 2, pp. 399–411, 2007.

[45] S. Abu-Abed, P. Dollé, D. Metzger, B. Beckett, P. Chambon, and M. Petkovich, “The retinoic acid-metabolizing enzyme, CYP26A1, is essential for normal hindbrain patterning, vertebral identity, and development of posterior structures,” *Genes Dev.*, vol. 15, no. 2, pp. 226–240, 2001.

[46] Y. Sakai *et al.*, “The retinoic acid-inactivating enzyme CYP26 is essential for establishing an uneven distribution of retinoic acid along the anterio-posterior axis within the mouse embryo,” *Genes Dev.*, vol. 15, no. 2, pp. 213–225, 2001.

[47] Y. Yokouchi, H. Sasaki, and A. Kuroiwa, “Homeobox gene expression correlated with the bifurcation process of limb cartilage development,” *Nature*, vol. 353, no. 6343, pp. 443–445, 1991.

[48] C. E. Nelson *et al.*, “Analysis of Hox gene expression in the chick limb bud,” *Development*, vol. 122, no. 5, pp. 1449–1466, 1996.

[49] N. Mercader *et al.*, “Ectopic Meis1 expression in the mouse limb bud alters P-D patterning in a Pbx1-independent manner,” *Int. J. Dev. Biol.*, vol. 53, no. 8–10, pp. 1483–

1494, 2009.

[50] N. Mercader, E. Leonardo, M. E. Piedra, C. Martinez-A., M. A. Ros, and M. Torres, "Opposing RA and FGF signals control proximodistal vertebrate limb development through regulation of Meis genes," *Development*, vol. 127, no. 18, pp. 3961–3970, 2000.

[51] K. L. Cooper, J. K. H. Hu, D. Ten Berge, M. Fernandez-Teran, M. A. Ros, and C. J. Tabin, "Initiation of proximal-distal patterning in the vertebrate limb by signals and growth," *Science (80-.).*, vol. 332, no. 6033, pp. 1083–1086, 2011.

[52] F. V. Mariani, C. P. Ahn, and G. R. Martin, "Genetic evidence that FGFs have an instructive role in limb proximal-distal patterning," *Nature*, vol. 453, no. 7193, pp. 401–405, 2008.

[53] T. J. Cunningham, X. Zhao, L. L. Sandell, S. M. Evans, P. A. Trainor, and G. Duester, "Antagonism between Retinoic Acid and Fibroblast Growth Factor Signaling during Limb Development," *Cell Rep.*, vol. 3, no. 5, pp. 1503–1511, 2013.

[54] A. Roselló-Díez, C. G. Arques, I. Delgado, G. Giovinazzo, and M. Torres, "Diffusible signals and epigenetic timing cooperate in late proximo-distal limb patterning," *Dev.*, vol. 141, no. 7, pp. 1534–1543, 2014.

[55] V. Dupé and A. Lumsden, "Hindbrain patterning involves graded responses to retinoic acid signalling," *Development*, vol. 128, no. 12, pp. 2199–2208, 2001.

[56] L. Maves and C. B. Kimmel, "Dynamic and sequential patterning of the zebrafish posterior hindbrain by retinoic acid," *Dev. Biol.*, vol. 285, no. 2, pp. 593–605, 2005.

[57] H. Marshall, S. Nonchev, M. H. Sham, I. Muchamore, A. Lumsden, and R. Krumlauf, "Retinoic acid alters hindbrain Hox code and induces transformation of rhombomeres 2/3 into a 4/5 identity," *Nature*, vol. 360, no. 6406, pp. 737–741, 1992.

[58] K. Niederreither, J. Vermot, B. Schuhbaur, P. Chambon, and P. Dollé, "Retinoic acid synthesis and hindbrain patterning in the mouse embryo," *Development*, vol. 127, no. 1, pp. 75–85, 2000.

[59] R. Neijts, S. Amin, C. van Rooijen, and J. Deschamps, "Cdx is crucial for the timing mechanism driving colinear Hox activation and defines a trunk segment in the Hox cluster topology," *Dev. Biol.*, vol. 422, no. 2, pp. 146–154, 2017.

[60] T. E. Foley, B. Hess, J. G. A. Savory, R. Ringuette, and D. Lohnes, "Role of Cdx factors in early mesodermal fate decisions.," *Development*, vol. 146, no. 7, p. dev170498, 2019.

[61] J. Chang, I. Skromne, and R. K. Ho, "CDX4 and retinoic acid interact to position the hindbrain-spinal cord transition," *Dev. Biol.*, vol. 410, no. 2, pp. 178–189, 2016.

[62] R. A. Wingert *et al.*, “The cdx genes and retinoic acid control the positioning and segmentation of the zebrafish pronephros,” *PLoS Genet.*, vol. 3, no. 10, pp. 1922–1938, 2007.

[63] P. M. Macdonald and G. Struhf, “A molecular gradient in early Drosophila embryos and its role in specify . ing the body pattern,” 1986.

[64] F. Beck, F. Tata, and K. Chawengsaksophak, “Homeobox genes and gut development,” *BioEssays*, vol. 22, no. 5, pp. 431–441, 2000.

[65] S. L. Pollard and P. W. H. Holland, “Evidence for 14 homeobox gene clusters in human genome ancestry,” vol. 4, pp. 1059–1062.

[66] P. W. H. Holland, “The ParaHox gene cluster is an evolutionary sister of the Hox gene cluster `,” vol. 392, no. April, pp. 61–63, 1998.

[67] E. O. Mazzoni *et al.*, “Saltatory remodeling of Hox chromatin in response to rostrocaudal patterning signals,” *Nat. Neurosci.*, vol. 16, no. 9, pp. 1191–1198, 2013.

[68] D. Beuchle, G. Struhl, and J. Müller, “Polycomb group proteins and heritable silencing of Drosophila Hox genes,” *Development*, vol. 128, no. 6, pp. 993–1004, 2001.

[69] T. Akasaka *et al.*, “Mice doubly deficient for the polycomb group genes Mel18 and Bmi1 reveal synergy and requirement for maintenance but not initiation of Hox gene expression,” *Development*, vol. 128, no. 9, pp. 1587–1597, 2001.

[70] D. Soshnikova, N. & Duboule, “Epigenetic Temporal Control of Mouse Hox Genes in Vivo,” *Science (80-.).*, no. June, pp. 1320–1324, 2009.

[71] M. P. Verzi *et al.*, “Differentiation-Specific Histone Modifications Reveal Dynamic Chromatin Interactions and Partners for the Intestinal Transcription Factor CDX2,” *Dev. Cell*, vol. 19, no. 5, pp. 713–726, 2010.

[72] M. Saxena, A. K. San Roman, N. K. O’Neill, R. Sulahian, U. Jadhav, and R. A. Shivdasani, “Transcription factor-dependent ‘anti-repressive’ mammalian enhancers exclude H3K27me3 from extended genomic domains,” *Genes Dev.*, vol. 31, no. 23–24, pp. 2391–2404, 2017.

[73] T. T. Nguyen *et al.*, “Cdx2 regulates gene expression through recruitment of Brg1-associated switch-sucrose non-fermentable (SWI-SNF) chromatin remodeling activity,” *J. Biol. Chem.*, vol. 292, no. 8, pp. 3389–3399, 2017.

[74] N. Yamamichi *et al.*, “Cdx2 and the Brm-type SWI/SNF complex cooperatively regulate villin expression in gastrointestinal cells,” *Exp. Cell Res.*, vol. 315, no. 10, pp. 1779–1789,

2009.

[75] V. Subramanian, B. I. Meyer, and P. Gruss, “Disruption of the murine homeobox gene Cdx1 affects axial skeletal identities by altering the mesodermal expression domains of Hox genes,” *Cell*, vol. 83, no. 4, pp. 641–653, 1995.

[76] E. van den Akker *et al.*, “Cdx1 and Cdx2 have overlapping functions in anteroposterior patterning and posterior axis elongation.,” *Development*, vol. 129, no. 9, pp. 2181–93, 2002.

[77] S. J. Gaunt, A. Cockley, and D. Drage, “Additional enhancer copies, with intact cdx binding sites, anteriorize Hoxa-7/lacZ expression in mouse embryos: Evidence in keeping with an instructional cdx gradient,” *Int. J. Dev. Biol.*, vol. 48, no. 7, pp. 613–622, 2004.

[78] S. J. Gaunt, D. Drage, and R. C. Trubshaw, “Increased Cdx protein dose effects upon axial patterning in transgenic lines of mice,” *Development*, vol. 135, no. 15, pp. 2511–2520, 2008.

[79] J. Tabaries S, Lapointe J, Besch T, Carter M, Woollard J, Tuggle CK, L., “Cdx Protein Interaction with Hoxa5 Regulatory Sequences Contributes to Hoxa5 Regional Expression along the Axial Skeleton,” *Mol Cell Biol*, vol. 25, no. 4, pp. 1–13, 2005.

[80] M. Mallo, D. M. Wellik, and J. Deschamps, “Hox genes and regional patterning of the vertebrate body plan,” *Dev. Biol.*, vol. 344, no. 1, pp. 7–15, 2010.

[81] A. J. Davidson and L. I. Zon, “The caudal-related homeobox genes cdx1a and cdx4 act redundantly to regulate hox gene expression and the formation of putative hematopoietic stem cells during zebrafish embryogenesis,” *Dev. Biol.*, vol. 292, no. 2, pp. 506–518, Apr. 2006.

[82] A. J. Davidson *et al.*, “Cdx4 Mutants Fail To Specify Blood Progenitors and Can Be Rescued By Multiple Hox Genes,” *Nature*, vol. 425, no. 6955, pp. 300–306, 2003.

[83] A. G. Hayward, P. Joshi, and I. Skromne, “Spatiotemporal analysis of zebrafish hox gene regulation by Cdx4,” *Dev. Dyn.*, vol. 244, no. 12, pp. 1564–1573, Dec. 2015.

[84] K. Chawengsaksophak, V. E. Hammond, and F. Beck, “Homeosis and intestinal tumours in Cdx2 mutant mice,” vol. 38616, no. March, pp. 4–7, 1997.

[85] K. Chawengsaksophak, W. De Graaff, J. Rossant, J. Deschamps, and F. Beck, “Cdx2 is essential for axial elongation in mouse development,” vol. 101, no. 20, pp. 7641–7645, 2004.

[86] J. van Nes, J., de Graaff, W., Lebrin, F., Gerhard, M., Beck, F. and Deschamps, “The Cdx4 mutation affects axial development and reveals an essential role of Cdx genes in the

ontogenesis of the placental labyrinth in mice," pp. 419–428, 2006.

[87] T. Young *et al.*, "Cdx and Hox Genes Differentially Regulate Posterior Axial Growth in Mammalian Embryos," *Dev. Cell*, vol. 17, no. 4, pp. 516–526, 2009.

[88] I. Skromne, D. Thorsen, M. Hale, V. E. Prince, and R. K. Ho, "Repression of the hindbrain developmental program by Cdx factors is required for the specification of the vertebrate spinal cord," *Development*, vol. 134, no. 11, pp. 2147–2158, May 2007.

[89] T. Shimizu, Y.-K. Bae, and M. Hibi, "Cdx-Hox code controls competence for responding to Fgfs and retinoic acid in zebrafish neural tissue," *Development*, vol. 133, no. 23, pp. 4709–4719, Nov. 2006.

[90] K. Lee and I. Skromne, "Retinoic acid regulates size, pattern and alignment of tissues at the head-trunk transition," *Development*, vol. 141, no. 22, pp. 4375–4384, 2014.

[91] M. Houle, P. Prinos, A. Iulianella, N. Bouchard, and D. Lohnes, "Retinoic Acid Regulation of Cdx1 : an Indirect Mechanism for Retinoids and Vertebral Specification," vol. 20, no. 17, pp. 6579–6586, 2000.

[92] D. Allan, M. Houle, N. Bouchard, B. I. Meyer, P. Gruss, and D. Lohnes, "RAR ⁄ and Cdx1 Interactions in Vertebral Patterning," vol. 60, pp. 46–60, 2001.

[93] H. Lickert and R. Kemler, "Functional Analysis of cis -Regulatory Elements Controlling Initiation and Maintenance of Early Cdx1 Gene Expression in the Mouse," vol. 220, no. July, pp. 216–220, 2002.

[94] P. Prinos, S. Joseph, K. Oh, B. I. Meyer, P. Gruss, and D. Lohnes, "Multiple Pathways Governing Cdx1 Expression during Murine Development," vol. 269, pp. 257–269, 2001.

[95] J. G. A. Savory *et al.*, "Cdx2 regulation of posterior development through non-Hox targets," *Development*, vol. 136, no. 24, pp. 4099–4110, 2009.

[96] E. J. Paik *et al.*, "A Cdx4-sall4 regulatory module controls the transition from mesoderm formation to embryonic hematopoiesis," *Stem Cell Reports*, vol. 1, no. 5, pp. 425–436, 2013.

[97] Y. Wang *et al.*, "Cdx gene deficiency compromises embryonic hematopoiesis in the mouse," *Proc. Natl. Acad. Sci. U. S. A.*, vol. 105, no. 22, pp. 7756–7761, 2008.

[98] T. Brooke-Bisschop, J. G. A. Savory, T. Foley, R. Ringuette, and D. Lohnes, "Essential roles for Cdx in murine primitive hematopoiesis," *Dev. Biol.*, vol. 422, no. 2, pp. 115–124, 2017.

[99] C. Lengerke *et al.*, "Interactions between Cdx genes and retinoic acid modulate early

cardiogenesis," *Dev. Biol.*, vol. 354, no. 1, pp. 134–142, 2011.

[100] P. Mohanty-Hejmadi, S. K. Dutta, and P. Mahapatra, "Limbs generated at site of tail amputation in marbled balloon frog after vitamin A treatment," *Nature*, vol. 355, no. 6358, pp. 352–353, 1992.

[101] J. C. Rutledge *et al.*, "Limb and lower-body duplications induced by retinoic acid in mice," *Proc. Natl. Acad. Sci. U. S. A.*, vol. 91, no. 12, pp. 5436–5440, 1994.

[102] M. W. Vandersea, P. Fleming, R. A. McCarthy, and D. G. Smith, "Fin duplications and deletions induced by disruption of retinoic acid signaling," *Dev. Genes Evol.*, vol. 208, no. 2, pp. 61–68, 1998.

[103] S. Chaube, "On axiation and symmetry in transplanted wing of the chick," *J. Exp. Zool.*, vol. 140, no. 1, pp. 29–77, 1959.

[104] B. R. Keegan, "Organization of cardiac chamber progenitors in the zebrafish blastula," *Development*, vol. 131, no. 13, pp. 3081–3091, 2004.

[105] J. J. Gibson-Brown *et al.*, "Evidence of a role for T-box genes in the evolution of limb morphogenesis and the specification of forelimb/hindlimb identity," *Mech. Dev.*, vol. 56, no. 1–2, pp. 93–101, 1996.

[106] P. Agarwal *et al.*, "Tbx5 is essential for forelimb bud initiation following patterning of the limb field in the mouse embryo.," *Development*, vol. 130, no. 3, pp. 623–33, 2003.

[107] D. G. Ahn, M. J. Kourakis, L. A. Rohde, L. M. Silvert, and R. K. Ho, "T-box gene Tbx5 is essential for formation of the pectoral limb bud," *Nature*, vol. 417, no. 6890, pp. 754–758, 2002.

[108] E. K. Don *et al.*, "Genetic basis of hindlimb loss in a naturally occurring vertebrate model," *Biol. Open*, vol. 5, no. 3, pp. 359–366, 2016.

[109] L. A. Naiche and V. E. Papaioannou, "Loss of Tbx4 blocks hindlimb development and affects vascularization and fusion of the allantois," *Development*, vol. 130, no. 12, pp. 2681–2693, 2003.

[110] C. Rallis *et al.*, "Tbx5 is required for forelimb bud formation and continued outgrowth," *Development*, vol. 130, no. 12, pp. 2741–2751, 2003.

[111] A. Isaac *et al.*, "Tbx genes and limb identity in chick embryo development," *Development*, vol. 125, no. 10, pp. 1867–1875, 1998.

[112] C. Minguillon, J. Del Buono, and M. P. Logan, "Tbx5 and Tbx4 are not sufficient to determine limb-specific morphologies but have common roles in initiating limb

outgrowth," *Dev. Cell*, vol. 8, no. 1, pp. 75–84, 2005.

[113] Q. Mao, H. K. Stinnett, and R. K. Ho, "Asymmetric cell convergence-driven zebrafish fin bud initiation and pre-pattern requires Tbx5a control of a mesenchymal Fgf signal," *Development*, vol. 142, no. 24, pp. 4329–4339, 2015.

[114] C. Moreau *et al.*, "Timed collinear activation of Hox genes during gastrulation controls the avian forelimb position," pp. 1–25, 2018.

[115] J. S. Waxman, B. R. Keegan, R. W. Roberts, K. D. Poss, and D. Yelon, "Hoxb5b Acts Downstream of Retinoic Acid Signaling in the Forelimb Field to Restrict Heart Field Potential in Zebrafish," *Dev. Cell*, vol. 15, no. 6, pp. 923–934, 2008.

[116] B. R. Keegan, J. L. Feldman, G. Begemann, P. W. Ingham, and D. Yelon, "Retinoic acid signaling restricts the cardiac progenitor pool," *Science (80-.).*, vol. 307, no. 5707, pp. 247–249, 2005.

[117] H. Grandel and M. Brand, "Zebrafish limb development is triggered by a retinoic acid signal during gastrulation," *Dev. Dyn.*, vol. 240, no. 5, pp. 1116–1126, 2011.

[118] Y. Gibert, "Induction and prepatterning of the zebrafish pectoral fin bud requires axial retinoic acid signaling," *Development*, vol. 133, no. 14, pp. 2649–2659, Jun. 2006.

[119] X. Zhao *et al.*, "Retinoic Acid Promotes Limb Induction through Effects on Body Axis Extension but Is Unnecessary for Limb Patterning," *Curr. Biol.*, vol. 19, no. 12, pp. 1050–1057, 2009.

[120] F. A. Mic, I. O. Sirbu, and G. Duester, "Retinoic acid synthesis controlled by Raldh2 is required early for limb bud initiation and then later as a proximodistal signal during apical ectodermal ridge formation," *J. Biol. Chem.*, vol. 279, no. 25, pp. 26698–26706, 2004.

[121] J. Partanen, L. Schwartz, and J. Rossant, "Opposite phenotypes of hypomorphic and Y766 phosphorylation site mutations reveal a function for Fgfr1 in anteroposterior patterning of mouse embryos," pp. 2332–2344, 1998.

[122] T. Stratford, C. Logan, M. Zile, and M. Maden, "Abnormal anteroposterior and dorsoventral patterning of the limb bud in the absence of retinoids," *Mech. Dev.*, vol. 81, no. 1–2, pp. 115–125, 1999.

[123] V. Dupé *et al.*, "Essential roles of retinoic acid signaling in interdigital apoptosis and control of BMP-7 expression in mouse autopods," *Dev. Biol.*, vol. 208, no. 1, pp. 30–43, 1999.

[124] S. Nishimoto, S. M. Wilde, S. Wood, and M. P. O. Logan, "RA Acts in a Coherent Feed-Forward Mechanism with Tbx5 to Control Limb Bud Induction and Initiation," *Cell Rep.*,

vol. 12, no. 5, pp. 879–891, 2015.

[125] N. Adachi, M. Robinson, A. Goolsbee, and N. H. Shubin, " Regulatory evolution of Tbx5 and the origin of paired appendages ," *Proc. Natl. Acad. Sci.*, vol. 113, no. 36, pp. 10115–10120, 2016.

[126] L. Ryckebusch *et al.*, "Retinoic acid deficiency alters second heart field formation," vol. 105, no. 8, 2008.

[127] M. R. J. Sorrell and J. S. Waxman, "Restraint of Fgf8 signaling by retinoic acid signaling is required for proper heart and forelimb formation," *Dev. Biol.*, vol. 358, no. 1, pp. 44–55, 2011.

[128] N. Mercader, S. Fischer, and C. J. Neumann, "Erratum: Prdm1 acts downstream of a sequential RA, Wnt and Fgf signaling cascade during zebrafish forelimb induction (Development (2006) vol. 133 (2805-2815))," *Development*, vol. 133, no. 19, p. 3949, 2006.

[129] J. K. Ng *et al.*, "The limb gene Tbx5 promotes limb initiation by interacting with Wnt2b adn Fgf10," *Development*, vol. 129, no. 22, pp. 5161–5170, 2002.

[130] J. Deschamps and J. van Nes, "Developmental regulation of the Hox genes during axial morphogenesis in the mouse," *Development*, vol. 132, no. 13, pp. 2931–2942, 2005.

[131] M. BATESON,WILLIAM, *STUDY OF VARIATION TREATED WITH ESPECIAL REGARD TO DISCONTINUITY IN THE ORIGIN OF SPECIES.* 1894.

[132] H. Genes, "Homeotic genes and the homeobox," 1986.

[133] W. Mcginnis, R. L. Garber, J. Wit-z, A. Kuroiwa, and W. J. Gehring, "A Homologous Protein-Coding Sequence in Drosophila Homeotic Genes and Its Conservation in Other Metazoans," vol. 37, no. June, pp. 403–408, 1984.

[134] D. Duboule and P. Dollé, "The structural and functional organization of the murine HOX gene family resembles that of Drosophila homeotic genes.," *EMBO J.*, vol. 8, no. 5, pp. 1497–1505, 1989.

[135] A. Graham, N. Papalopulu, and R. Krumlauf, "The murine and Drosophila homeobox gene complexes have common features of organization and expression," *Cell*, vol. 57, no. 3, pp. 367–378, 1989.

[136] A. C. Burke, C. E. Nelson, B. A. Morgan, and C. Tabin, "Hox genes and the evolution of vertebrate axial morphology.," *Development*, vol. 121, no. 2, pp. 333–46, 1995.

[137] M. Kessel, R. Balling, and P. Gruss, "Variations of cervical vertebrate after expression of

a Hox-1.1 transgene in mice," *Cell*, vol. 61, no. 2, pp. 301–308, 1990.

[138] B. G. Jegalian and E. M. De Robertis, "Homeotic transformations in the mouse induced by overexpression of a human Hox3.3 transgene," *Cell*, vol. 71, no. 6, pp. 901–910, 1992.

[139] R. A. Pollock, G. Jay, and C. J. Bieberich, "Altering the boundaries of Hox3.1 expression: Evidence for antipodal gene regulation," *Cell*, vol. 71, no. 6, pp. 911–923, 1992.

[140] A. Carapuco, N. Novoa, N. Bobola, and M. Mallo, "Hox genes specify vertebral types in the presomitic mesodermAna," *Genes Dev.*, pp. 2116–2121, 2005.

[141] D. M. Wellik and M. R. Capecchi, "Hox10 and Hox11 genes are required to globally pattern the mammalian skeleton," *Science (80-.).*, vol. 301, no. 5631, pp. 363–367, 2003.

[142] H. Le Mouellic, Y. Lallemand, and P. Brûlet, "Homeosis in the mouse induced by a null mutation in the Hox-3.1 gene," *Cell*, vol. 69, no. 2, pp. 251–264, 1992.

[143] X. He *et al.*, "MiR-196 regulates axial patterning and pectoral appendage initiation," *Dev. Biol.*, vol. 357, no. 2, pp. 463–477, 2011.

[144] D. E. Rancourt, T. Tsuzuki, and M. R. Capecchi, "Genetic interaction between hoxb-5 and hoxb-6 is revealed by nonallelic noncomplementation," *Genes Dev.*, vol. 9, no. 1, pp. 108–122, Jan. 1995.

[145] B. Xu *et al.*, "Hox5 interacts with Plzf to restrict Shh expression in the developing forelimb," *Proc. Natl. Acad. Sci. U. S. A.*, vol. 110, no. 48, pp. 19438–19443, 2013.

[146] B. Xu and D. M. Wellik, "Axial Hox9 activity establishes the posterior field in the developing forelimb," *Proc. Natl. Acad. Sci.*, vol. 108, no. 12, pp. 4888–4891, 2011.

[147] M. Kessel and P. Gruss, "Homeotic Transformations of Murine Vertebrae and Concomitant Alteration of Hox Codes Induced by Retinoic Acid," *Cell*, vol. 67, no. 1894, 1991.

[148] M. Balling, R., Mutter, G., Gruss, P., and Kessel, "Craniofacial Abnormalities Induced by Ectopic Expression of the Homeobox Gene Hox1.1 in Transgenic Mice," vol. 58, pp. 337–347, 1999.

[149] G. M. Morriss-Kay, P. Murphy, R. E. Hill, and D. R. Davidson, "Effects of retinoic acid excess on expression of Hox-2.9 and Krox-20 and on morphological segmentation in the hindbrain of mouse embryos.," *EMBO J.*, vol. 10, no. 10, pp. 2985–2995, 1991.

[150] R. A. Conlon and J. Rossant, "Exogenous retinoic acid rapidly induces anterior ectopic expression of murine Hox-2 genes in vivo," *Development*, vol. 116, no. 2, pp. 357–368, 1992.

[151] C. B. Kimmel, W. W. Ballard, S. R. Kimmel, B. Ullmann, and T. F. Schilling, “Stages of embryonic development of the zebrafish,” *Dev. Dyn.*, vol. 203, no. 3, pp. 253–310, 1995.

[152] O. H. Ocaña *et al.*, “A right-handed signalling pathway drives heart looping in vertebrates,” *Nature*, vol. 549, no. 7670, pp. 86–90, 2017.

[153] C. McMahon, G. Gestri, S. W. Wilson, and B. A. Link, “Lmx1b is essential for survival of periocular mesenchymal cells and influences Fgf-mediated retinal patterning in zebrafish,” *Dev. Biol.*, vol. 332, no. 2, pp. 287–298, 2009.

[154] M. Akimenko, M A; Ekker, “Anterior Duplication of the Sonic hedgehog Expression Pattern in the Pectoral Fin Buds of Zebrafish Treated with Retinoic Acid,” *Dev. Biol.*, 1995.

[155] V. E. Prince, L. Joly, M. Ekker, and R. K. Ho, “Zebrafish hox genes: Genomic organization and modified colinear expression patterns in the trunk,” *Development*, vol. 125, no. 3, pp. 407–420, 1998.

[156] S. Schulte-Merker, R. K. Ho, B. G. Herrmann, and C. Nusslein-Volhard, “The protein product of the zebrafish homologue of the mouse T gene is expressed in nuclei of the germ ring and the notochord of the early embryo,” *Development*, vol. 116, no. 4, pp. 1021–1032, 1992.

[157] T. J. Cunningham and G. Duester, “Mechanisms of retinoic acid signalling and its roles in organ and limb development,” *Nat. Rev. Mol. Cell Biol.*, vol. 16, no. 2, pp. 110–123, 2015.

[158] Y. Emoto, H. Wada, H. Okamoto, A. Kudo, and Y. Imai, “Retinoic acid-metabolizing enzyme Cyp26a1 is essential for determining territories of hindbrain and spinal cord in zebrafish,” *Dev. Biol.*, vol. 278, no. 2, pp. 415–427, 2005.

[159] G. Begemann and P. W. Ingham, “Developmental regulation of Tbx5 in zebrafish embryogenesis,” *Mech. Dev.*, vol. 90, no. 2, pp. 299–304, 2000.

[160] C. Gros, Jerome and Tabin,J, “Vertebrate Limb bud formation is initiated by localized Epithelial to Mesenchymal Transition,” *Science (80-.).*, vol. 23, no. 1, pp. 1–7, 2014.

[161] P.-Y. Cheng *et al.*, “Zebrafish cdx1b regulates expression of downstream factors of Nodal signaling during early endoderm formation,” *Development*, vol. 135, no. 5, pp. 941–952, 2008.

[162] J. L. O. De Jong *et al.*, “Interaction of retinoic acid and scl controls primitive blood development,” *Blood*, vol. 116, no. 2, pp. 201–209, Jul. 2010.

[163] M. D. Kinkel, S. C. Eames, M. R. Alonzo, and V. E. Prince, “Cdx4 is required in the

endoderm to localize the pancreas and limit -cell number," *Development*, vol. 135, no. 5, pp. 919–929, 2008.

[164] X. Gu, F. Xu, X. Wang, X. Gao, and Q. Zhao, "Molecular cloning and expression of a novel CYP26 gene (cyp26d1) during zebrafish early development," *Gene Expr. Patterns*, vol. 5, no. 6, pp. 733–739, Aug. 2005.

[165] Q. Zhao, B. Dobbs-McAuliffe, and E. Linney, "Expression of cyp26b1 during zebrafish early development," *Gene Expr. Patterns*, vol. 5, no. 3, pp. 363–369, 2005.

[166] S. Anbalagan *et al.*, "Pituicyte Cues Regulate the Development of Permeable Neuro-Vascular Interfaces," *Dev. Cell*, vol. 47, no. 6, pp. 711-726.e5, 2018.

[167] H. Grandel and S. Schulte-Merker, "The development of the paired fins in the Zebrafish (Danio rerio)," *Mech. Dev.*, vol. 79, pp. 99 – 120, 1998.

[168] M. Berenguer, J. J. Lancman, T. J. Cunningham, P. D. S. Dong, and G. Duester, "Mouse but not zebrafish requires retinoic acid for control of neuromesodermal progenitors and body axis extension," *Dev. Biol.*, vol. 441, no. 1, pp. 127–131, 2018.

[169] A. B. Rydeen and J. S. Waxman, "Cyp26 enzymes are required to balance the cardiac and vascular lineages within the anterior lateral plate mesoderm," *Development*, vol. 141, no. 8, pp. 1638–1648, 2014.

[170] J. J. Schoenebeck, B. R. Keegan, and D. Yelon, "Vessel and Blood Specification Override Cardiac Potential in Anterior Mesoderm," *Dev. Cell*, vol. 13, no. 2, pp. 254–267, 2007.

[171] L. A. Wyngaarden, K. M. Vogeli, B. G. Ciruna, M. Wells, A.-K. Hadjantonakis, and S. Hopyan, "Oriented cell motility and division underlie early limb bud morphogenesis," *J. Cell Sci.*, vol. 123, no. 15, pp. e1–e1, 2010.

[172] S. Fischer, B. W. Draper, and C. J. Neumann, "The zebrafish fgf24 mutant identifies and additional level of Fgf signaling involved in vertebrate forelimb initiation," *Development*, vol. 130, no. 15, pp. 3515–3524, 2003.

[173] B. Punnamoottil, H. Kikuta, G. Pezeron, J. Erceg, T. S. Becker, and S. Rinkwitz, "Enhancer detection in zebrafish permits the identification of neuronal subtypes that express Hox4 paralogs," *Dev. Dyn.*, vol. 237, no. 8, pp. 2195–2208, 2008.

[174] D. Lohnes, "The Cdx1 homeodomain protein : an integrator of posterior signaling in the mouse," pp. 971–980, 2003.

[175] M. J. Cohn, K. Patel, R. Krumlauf, D. G. Wilkinsont, J. D. W. Clarke, and C. Tickle, "Hox9 genes and vertebrate limb specification," *Nature*, vol. 387, no. 6628, pp. 97–101, 1997.

[176] M. J. Cohn and C. Tickle, “letters to nature Developmental basis of limblessness and axial patterning in snakes anterior posterior,” vol. 399, no. JUNE, 1999.

[177] C. Minguillon, S. Nishimoto, S. Wood, E. Vendrell, J. J. Gibson-Brown, and M. P. O. Logan, “Hox genes regulate the onset of Tbx5 expression in the forelimb,” *Development*, vol. 139, no. 17, pp. 3180–3188, 2012.

[178] S. Nishimoto, C. Minguillon, S. Wood, and M. P. O. Logan, “A Combination of Activation and Repression by a Colinear Hox Code Controls Forelimb-Restricted Expression of Tbx5 and Reveals Hox Protein Specificity,” *PLoS Genet.*, vol. 10, no. 3, pp. 1–13, 2014.

[179] S. Ueda *et al.*, “ Cux2 refines the forelimb field by controlling expression of Raldh2 and Hox genes ,” *Biol. Open*, vol. 8, no. 2, p. bio040584, 2019.

[180] D. Yelon *et al.*, “The bHLH transcription factor hand2 plays parallel roles in zebrafish heart and pectoral fin development.,” *Development*, vol. 127, no. 12, pp. 2573–82, 2000.

[181] F. A. Mic, R. J. Haselbeck, A. E. Cuenca, and G. Duester, “Novel retinoic acid generating activities in the neural tube and heart identified by conditional rescue of Raldh2 null mutant mice,” *Development*, vol. 129, no. 9, pp. 2271–2282, 2002.

[182] A. Molotkov, N. Molotkova, and G. Duester, “Retinoic acid guides eye morphogenetic movements via paracrine signaling but is unnecessary for retinal dorsoventral patterning,” *Development*, vol. 133, no. 10, pp. 1901–1910, 2006.

[183] G. A. Hyatt, E. A. Schmitt, N. R. Marsh-Armstrong, and J. E. Dowling, “Retinoic acid-induced duplication of the zebrafish retina,” *Proc. Natl. Acad. Sci. U. S. A.*, vol. 89, no. 17, pp. 8293–8297, 1992.

[184] B. L. Martin and D. Kimelman, “Brachyury establishes the embryonic mesodermal progenitor niche,” *Genes Dev.*, vol. 24, no. 24, pp. 2778–2783, 2010.

[185] T. M. Jessell, “Neuronal specification in the spinal cord: Inductive signals and transcriptional codes,” *Nat. Rev. Genet.*, vol. 1, no. 1, pp. 20–29, 2000.

[186] J. S. Dasen, J. P. Liu, and T. M. Jessell, “Motor neuron columnar fate imposed by sequential phases of Hox-c activity,” *Nature*, vol. 425, no. 6961, pp. 926–933, 2003.

[187] H. Jung *et al.*, “Evolving hox activity profiles govern diversity in locomotor systems,” *Dev. Cell*, vol. 29, no. 2, pp. 171–187, 2014.

[188] J. S. Dasen, B. C. Tice, S. Brenner-Morton, and T. M. Jessell, “A Hox regulatory network establishes motor neuron pool identity and target-muscle connectivity,” *Cell*, vol. 123, no.

3, pp. 477–491, 2005.

[189] L. H. Ma, E. Gilland, A. H. Bass, and R. Baker, “Ancestry of motor innervation to pectoral fin and forelimb,” *Nat. Commun.*, vol. 1, no. 4, pp. 1–8, 2010.

[190] A. Chevallier, M. Kieny, and A. Mauger, “Limb-somite relationship: origin of the limb musculature,” *J. Embryol. Exp. Morphol.*, vol. Vol.41, no. 1951, pp. 245–258, 1977.

[191] J. C. Talbot, E. M. Teets, D. Ratnayake, P. Q. Duy, P. D. Currie, and S. L. Amacher, “Muscle precursor cell movements in zebrafish are dynamic and require Six family genes,” *Development*, vol. 146, no. 10, 2019.

[192] D. E. Rosen, “Teleostean interrelationships, morphological function and evolutionary inference,” *Integr. Comp. Biol.*, vol. 22, no. 2, pp. 261–273, 1982.

[193] H. Grandel and S. Schulte-Merker, “The development of the paired fins in the zebrafish (Danio rerio),” *Mech. Dev.*, vol. 79, no. 1–2, pp. 99–120, 1998.

[194] M. Tanaka, “Revealing the mechanisms of the rostral shift of pelvic fins among teleost fishes,” *Evol. Dev.*, vol. 13, no. 4, pp. 382–390, 2011.

[195] M. Tanaka *et al.*, “Developmental genetic basis for the evolution of pelvic fin loss in the pufferfish Takifugu rubripes,” *Dev. Biol.*, vol. 281, no. 2, pp. 227–239, 2005.

[196] H. Kaneko, Y. Nakatani, K. Fujimura, and M. Tanaka, “Development of the lateral plate mesoderm in medaka Oryzias latipes and Nile tilapia Oreochromis niloticus: Insight into the diversification of pelvic fin position,” *J. Anat.*, vol. 225, no. 6, pp. 659–674, 2014.

[197] V. Lecaudey, G. Cakan-Akdogan, W. H. J. Norton, and D. Gilmour, “Dynamic Fgf signaling couples morphogenesis and migration in the zebrafish lateral line primordium,” *Development*, vol. 135, no. 16, pp. 2695–2705, 2008.

[198] S. Ota, N. Tonou-Fujimori, and K. Yamasu, “The roles of the FGF signal in zebrafish embryos analyzed using constitutive activation and dominant-negative suppression of different FGF receptors,” *Mech. Dev.*, vol. 126, no. 1–2, pp. 1–17, 2009.

[199] M. Tanaka, R. Yu, and D. Kurokawa, “Anterior migration of lateral plate mesodermal cells during embryogenesis of the pufferfish takifugu niphobles: Insight into the rostral positioning of pelvic fins,” *J. Anat.*, vol. 227, no. 1, pp. 81–88, 2015.

[200] B. Christen, A. M. C. Rodrigues, M. B. Monasterio, C. F. Roig, and J. C. I. Belmonte, “Transient downregulation of Bmp signalling induces extra limbs in vertebrates,” *Dev.*, vol. 139, no. 14, pp. 2557–2565, 2012.

[201] R. Jovelin *et al.*, “Evolution of developmental regulation in the vertebrate FgfD subfamily,” *J. Exp. Zool. Part B Mol. Dev. Evol.*, vol. 314, no. 1 B, pp. 33–56, 2010.

[202] P. R. Biga *et al.*, "The isolation, characterization, and expression of a novel GDF11 gene and a second myostatin form in zebrafish, Danio rerio," *Comp. Biochem. Physiol. - B Biochem. Mol. Biol.*, vol. 141, no. 2, pp. 218–230, 2005.

[203] C. Xu, G. Wu, Y. Zohar, and S. J. Du, "Analysis of myostatin gene structure, expression and function in zebrafish," *J. Exp. Biol.*, vol. 206, no. 22, pp. 4067–4079, 2003.

[204] M. Mallo, "Reassessing the Role of Hox Genes during Vertebrate Development and Evolution," *Trends Genet.*, vol. 34, no. 3, pp. 209–217, 2018.

[205] A. C. McPherron, A. M. Lawler, and S. J. Lee, "Regulation of anterior/posterior patterning of the axial skeleton by growth/differentiation factor 11," *Nat. Genet.*, vol. 22, no. 3, pp. 260–264, 1999.

[206] A. D. Jurberg, R. Aires, I. Varela-Lasheras, A. Nóvoa, and M. Mallo, "Switching axial progenitors from producing trunk to tail tissues in vertebrate embryos," *Dev. Cell*, vol. 25, no. 5, pp. 451–462, 2013.

[207] Y. Nakajima, M. Sakabe, H. Matsui, H. Sakata, N. Yanagawa, and T. Yamagishi, "Heart development before beating," *Anat. Sci. Int.*, vol. 84, no. 3, pp. 67–76, 2009.

[208] D. Ye, H. Xie, B. Hu, and F. Lin, "Endoderm convergence controls subduction of the myocardial precursors during heart-tube formation," *Dev.*, vol. 142, no. 17, pp. 2928–2940, 2015.

[209] V. D. Varner and L. A. Taber, "Not just inductive: A crucial mechanical role for the endoderm during heart tube assembly," *Development*, vol. 139, no. 9, pp. 1680–1690, 2012.

[210] J. F. Reiter *et al.*, "Gata5 is required for the development of the heart and endoderm in zebrafish," *Genes Dev.*, vol. 13, no. 22, pp. 2983–2995, 1999.